

Computational modelling and experimental study of the thermal transport characteristics of graphene nanoribbons

Junjie Chen¹

¹Department of Energy and Power Engineering, School of Mechanical and Power Engineering, Henan Polytechnic University, Jiaozuo, Henan, 454000, P.R. China. *
Corresponding author, E-mail address: cjjtpj@163.com,
<https://orcid.org/0000-0002-4222-1798>

February 17, 2023

Abstract

Graphene is a two-dimensional form of crystalline carbon, either a single layer of carbon atoms forming a hexagonal lattice or several coupled layers of this honeycomb structure. Graphene is a parent form of all graphitic structures of carbon. However, the field of graphene science and technology is relatively new. Progress depends not only on the basic science but also on the development of new ways to produce graphene on an industrial scale. The present study is focused primarily upon the thermal transport characteristics of graphene nanoribbons. The thermal transport characteristics of graphene nanoribbons are studied using molecular dynamics simulations and by experimental measurements. A specific heat flux is imposed through the graphene nanoribbon. The graphene nanoribbon is considered as a single layer of carbon atoms with each atom bound to three neighbors in a honeycomb structure. The thermal conductivity is determined from the temperature gradient obtained and the heat flux imposed. The present study aims to provide a fundamental understanding of the thermal transport properties of graphene nanoribbons. Particular emphasis is placed upon the effect of various factors on the thermal conductivity of graphene nanoribbons under different conditions. The results indicate that the mean free path of phonons depends on the nanoribbon structure and dimensions. The thermal conductivity increases with increasing nanoribbon length. Graphene nanoribbons offer tremendous promise for providing enhanced transport performance. Graphene undergoes a metallic-to-semiconducting transition as the nanoribbon width decreases. The properties of graphene nanoribbons are highly dependent on their width and edge structure. The graphene nanoribbons can be derived through the longitudinal splitting of carbon nanotubes.

Keywords: Graphene nanoribbons; Graphitic structures; Carbon nanotubes; Carbon nanofibers; Thermal properties; Thermal conductivity

Computational modelling and experimental study of the thermal transport characteristics of graphene nanoribbons

Junjie Chen

Department of Energy and Power Engineering, School of Mechanical and Power Engineering, Henan Polytechnic University, Jiaozuo, Henan, 454000, P.R. China

* Corresponding author, E-mail address: cjjtpj@163.com, <https://orcid.org/0000-0002-4222-1798>

Abstract

Graphene is a two-dimensional form of crystalline carbon, either a single layer of carbon atoms forming a hexagonal lattice or several coupled layers of this honeycomb structure. Graphene is a parent form of all graphitic structures of carbon. However, the field of graphene science and technology is relatively new. Progress depends not only on the basic science but also on the development of new ways to produce graphene on an industrial scale. The present study is focused primarily upon the thermal transport characteristics of graphene nanoribbons. The thermal transport characteristics of graphene nanoribbons are studied using

molecular dynamics simulations and by experimental measurements. A specific heat flux is imposed through the graphene nanoribbon. The graphene nanoribbon is considered as a single layer of carbon atoms with each atom bound to three neighbors in a honeycomb structure. The thermal conductivity is determined from the temperature gradient obtained and the heat flux imposed. The present study aims to provide a fundamental understanding of the thermal transport properties of graphene nanoribbons. Particular emphasis is placed upon the effect of various factors on the thermal conductivity of graphene nanoribbons under different conditions. The results indicate that the mean free path of phonons depends on the nanoribbon structure and dimensions. The thermal conductivity increases with increasing nanoribbon length. Graphene nanoribbons offer tremendous promise for providing enhanced transport performance. Graphene undergoes a metallic-to-semiconducting transition as the nanoribbon width decreases. The properties of graphene nanoribbons are highly dependent on their width and edge structure. The graphene nanoribbons can be derived through the longitudinal splitting of carbon nanotubes.

Keywords: Graphene nanoribbons; Graphitic structures; Carbon nanotubes; Carbon nanofibers; Thermal properties; Thermal conductivity

1. Introduction

Elemental carbon exists in several forms, each of which has its own physical characteristics. Two of its well-defined forms, diamond and graphite, are crystalline in structure, but they differ in physical properties because the arrangements of the atoms in their structures are dissimilar. A third form, called fullerene, consists of a variety of molecules composed entirely of carbon. Spheroidal, closed-cage fullerenes are called buckminsterfullerenes, or buckyballs, and cylindrical fullerenes are called carbon nanotubes. Carbon has five unique crystalline structures, namely diamond, fullerene, carbon nanotubes or carbon nanofibers, graphene, and graphite [1, 2]. Fullerene is a zero-dimensional nano-graphitic material [3]. Carbon nanotubes and carbon nanofibers are a one-dimensional nanocarbon or nano-graphitic material [4]. Carbon nanotubes and carbon nanofibers have a diameter on the order of a few nanometers to a few hundred nanometers. Their longitudinal, hollow structures impart unique chemical, electrical, and mechanical properties to the material [5, 6]. Graphene is a two-dimensional nano-graphitic material and graphite is a three-dimensional graphitic material.

Bulk natural graphite is a three-dimensional graphitic material, and each graphite particle is composed of multiple grains with grain boundaries that demarcate adjacent graphite single crystals. Each grain is composed of multiple graphene planes that are oriented parallel to each other. A graphene plane in a graphite crystallite is composed of carbon atoms occupying a two-dimensional, hexagonal lattice [7, 8]. In a given grain or single crystal, the graphene planes are stacked and bonded through van der Waal forces in a direction perpendicular to the graphene plane. Although all the graphene planes in one grain are parallel to each other, typically the graphene planes in one grain and the graphene planes in an adjacent grain are inclined at different orientations [9, 10]. This means that the orientations of the various grains in a graphite particle typically differ from each other.

A graphite single crystal per se is anisotropic with a property measured along a direction in the basal plane being dramatically different than if measured along the crystallographic *c*-axis direction [11, 12]. For instance, the thermal conductivity of a graphite single crystal can be up to approximately 1,920 W / (m·K) or approximately 1,800 W / (m·K) in the basal plane [13, 14], but that along the crystallographic *c*-axis direction is less than approximately 10 W / (m·K) [15, 16]. Further, the multiple grains or crystallites in a graphite particle are typically all oriented along different and random directions [17, 18]. Consequently, a natural graphite particle composed of multiple grains of different orientations exhibits an average property between these two extremes.

It would be highly desirable in many applications to produce a graphitic film containing single or multiple graphene grains, having sufficiently large dimensions and having all graphene planes being essentially parallel to one another along one desired direction [19, 20]. In other words, it is highly desirable to have one large-size graphitic film having the *c*-axis directions of all the graphene planes being substantially parallel to one

another and having a sufficiently large film length and width for a particular application [21, 22]. It has not been possible to produce such a highly oriented graphitic film [23, 24]. Even though some attempts have been made to produce the so-called highly oriented pyrolytic graphite through tedious, energy intensive, and expensive chemical vapor deposition followed by ultra-high temperature graphitization [25, 26], the graphitic structure of the highly oriented pyrolytic graphite remains inadequately aligned and laden with defects and, hence, exhibits properties that are significantly lower than what are theoretically predicted.

The constituent graphene planes of a graphite crystallite in a natural or artificial graphite particle can be exfoliated and extracted or isolated to obtain individual graphene sheets of carbon atoms provided the interplanar van der Waals forces can be overcome [27, 28]. An isolated, individual graphene sheet of carbon atoms is commonly referred to as single-layer graphene [29, 30]. A stack of multiple graphene planes bonded through van der Waals forces in the thickness direction with an inter-graphene plane spacing of approximately 0.3354 nanometers is commonly referred to as a multi-layer graphene [31, 32]. A multi-layer graphene platelet has up to 300 layers of graphene planes, but more typically up to 30 graphene planes, even more typically up to 20 graphene planes, and most typically up to 10 graphene planes [33, 34]. Single-layer graphene and multi-layer graphene sheets are collectively called nanographene platelets [35, 36]. Graphene or graphene oxide sheets or platelets are a new class of carbon nanomaterial that is distinct from the zero-dimensional fullerene, the one-dimensional carbon nanotubes, and the three-dimensional graphite.

Graphene is a two-dimensional form of crystalline carbon, either a single layer of carbon atoms forming a hexagonal lattice or several coupled layers of this honeycomb structure. Graphene is a parent form of all graphitic structures of carbon. However, the field of graphene science and technology is relatively new. Progress depends not only on the basic science but also on the development of new ways to produce graphene on an industrial scale. The present study is focused primarily upon the thermal transport characteristics of graphene nanoribbons. The thermal transport characteristics of graphene nanoribbons are studied using molecular dynamics simulations and by experimental measurements. A specific heat flux is imposed through the graphene nanoribbon. The graphene nanoribbon is considered as a single layer of carbon atoms with each atom bound to three neighbors in a honeycomb structure. The thermal conductivity is determined from the temperature gradient obtained and the heat flux imposed. The present study aims to provide a fundamental understanding of the thermal transport properties of graphene nanoribbons. Particular emphasis is placed upon the effect of various factors on the thermal conductivity of graphene nanoribbons under different conditions.

2. Methods

The honeycomb lattice of graphene actually consists of two sublattices, designated A and B, such that each atom in sublattice A is surrounded by three atoms of sublattice B and vice versa. This simple geometrical arrangement leads to the appearance that the electrons and holes in graphene have an unusual degree of internal freedom, usually called pseudospin. In fact, making the analogy more complete, pseudospin mimics the spin, or internal angular momentum, of subatomic particles. Within this analogy, electrons and holes in graphene play the same role as particles and antiparticles in quantum electrodynamics. This makes graphene a test bed for high-energy physics: some quantum relativistic effects that are hardly reachable in experiments with subatomic particles using particle accelerators have clear analogs in the physics of electrons and holes in graphene, which can be measured and studied more easily because of their lower velocity. Thus, graphene provides a bridge between materials science and some areas of fundamental physics.

There is another reason why graphene is of special interest to fundamental science. Graphene is the first and simplest example of a two-dimensional crystal, that is, a solid material that contains just a single layer of atoms arranged in an ordered pattern. Two-dimensional systems are of huge interest not only for physics and chemistry but also for other natural sciences. In many respects, two-dimensional systems are fundamentally different from three-dimensional systems. In particular, due to very strong thermal fluctuations of atomic positions that remain correlated at large distances, long-range crystalline order cannot exist in two dimensions. Instead, only short-range order exists, and it does so only on some finite scale of characteristic length, a caveat that should be noted when graphene is called a two-dimensional crystal. For this reason, two-

dimensional systems are inherently flexural, manifesting strong bending fluctuations, so that they cannot be flat and are always rippled or corrugated. Graphene, because of its relative simplicity, can be considered as a model system for studying two-dimensional physics and chemistry in general. Other two-dimensional crystals besides graphene can be derived by exfoliation from other multilayer crystals, for example, hexagonal boron nitride, molybdenum disulfide, or tungsten disulfide, or by chemical modification of graphene, for example, hydrogenated graphene, or fluorinated graphene. Modern electronics are basically two-dimensional in that they use mainly the surface of semiconducting materials. Therefore, graphene and other two-dimensional materials are considered very promising for many such applications. Using graphene, for example, it should be possible to make electronic devices that are much thinner than devices made of traditional materials. Graphene does not have an insulator state, and conductivity remains finite at any doping.

The thermal transport characteristics of graphene nanoribbons are studied using molecular dynamics simulations. A specific heat flux imposed through the graphene nanoribbon modeled in this study is depicted schematically in Figure 1 in a shape of rectangle. The graphene nanoribbon is monolayer and thus can be considered as a single layer of carbon atoms with each atom bound to three neighbors in a honeycomb structure. The substantially flat monolayer of carbon atoms is usually referred to as the basal plane of the graphene nanoribbon. The monolayer graphene nanoribbon includes an edge irregularity, such as a zig-zag configuration edge or an armchair-configuration edge. The transverse edges at both ends of the graphene nanoribbon are rough, whereas the longitudinal edges at both sides of the graphene nanoribbon are substantially smooth. It is worth noting that the direction of heat flow is perpendicular to the irregularly shaped edges of the graphene nanoribbon. The transverse edges at both ends of the nanostructured graphene nanoribbon are atomically-disordered in the form of roughness. This edge disorder can degrade the thermal, electronic, and structural properties of the nanostructured graphene nanoribbon, including its electron mobility and strength. The graphene nanoribbon has a generally square shape with the width approximately equal to the length. The graphene nanoribbon has a generally square shape with the width approximately equal to the length.

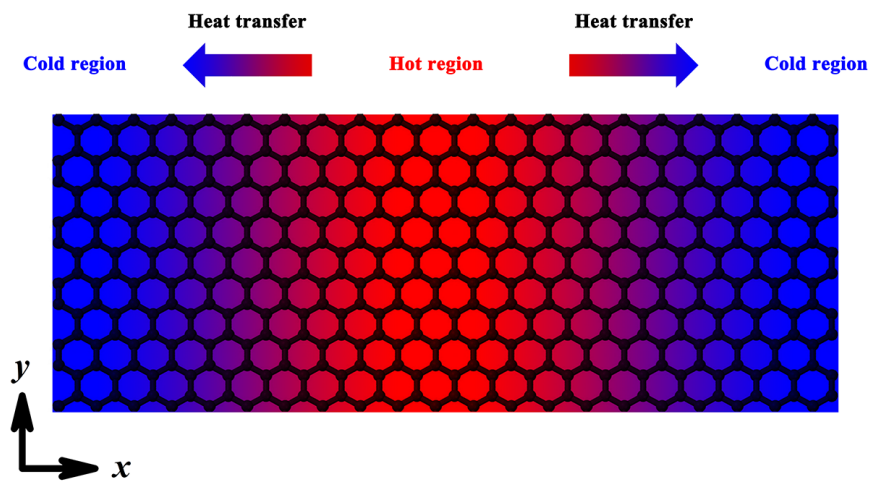


Figure 1. Schematic diagram of a specific heat flux imposed through one individual graphene nanoribbon in a shape of rectangle. It is assumed and indicated that the property being transported in the graphene nanoribbon flows from the red region to the blue regions. Linear momentum of the atoms is transferred to maintain a constant heat flux between the red region and the blue regions.

The length of the monolayer graphene nanoribbon is typically significantly greater than its width, but of course, there are exceptions. A specific heat flux imposed through the graphene nanoribbon modeled in this study is depicted schematically in Figure 2 in a shape of square. Unless otherwise stated, the graphene

nanoribbon is 5.4 nanometers in width, 40 nanometers in length, and 0.335 nanometers in thickness. The structure of the graphene nanoribbon is divided into specific regions by defining hot and cold slabs. Heat is continually being transferred from the hot slab to the cold slabs so as to equalize the temperature within the graphene nanoribbon. The temperature gradient can be determined in the direction of heat flow, since the total energy is conserved in the heat conduction process. Accordingly, the thermal conductivity can be determined from the temperature gradient obtained and the heat flux imposed. The basic rate equation of the heat conduction process within the graphene nanoribbon is known as Fourier’s law of heat conduction. The ratio of heat flux to the slope of the temperature profile is proportional to the thermal conductivity of the graphene nanoribbon. Fourier’s Law therefore provides the definition of the thermal conductivity of the graphene nanoribbon, and forms the basis of the general method that can be used to determine its value. The thermal conductivity of the monolayer graphene nanoribbon is proportional to the effective mean free path for phonon scattering. Therefore, the thermal conductivity variation over a range of the effective mean free path for phonon scattering can be represented as a straight line. Additionally, the intrinsic thermal conductivity of the two-dimensional carbon-based material can be derived from the intercept of the straight line by extrapolation from the case with infinite length.

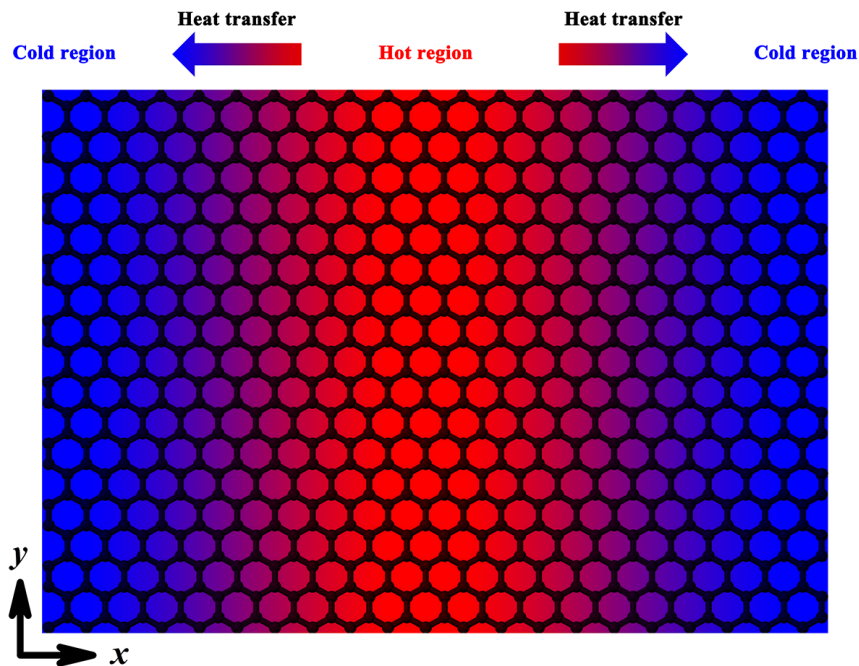


Figure 2. Schematic diagram of a specific heat flux imposed through one individual graphene nanoribbon in a shape of square. The red region has a higher value of temperature than the blue regions and that the property being transported in the graphene nanoribbon therefore flows from the red region to the blue regions. The arrows indicate the direction of heat transfer between the hot and cold regions. Linear momentum of the atoms is transferred to maintain a constant heat flux between the red region and the blue regions and a constant temperature gradient across the graphene nanoribbon.

Graphite generally comprises multiple layers of carbon atoms arranged in planar hexagonal lattices. In its highly oriented pyrolytic form, the hexagonal lattice sheets have an angular spread of less than one degree. This structure results in properties that are highly desirable for use in vacuum electron devices. For example, highly oriented pyrolytic graphite is well suited for use as a vacuum barrier. When used to manufacture components that form part of the vacuum seal, highly oriented pyrolytic graphite maintains vacuum integrity. Highly oriented pyrolytic graphite also possesses the lowest sputtering rate of all materials. Thus,

electrodes made from highly oriented pyrolytic graphite will emit far fewer contaminating trace elements during operation than will copper or molybdenum electrodes. Further contributing to this property is that fact that highly oriented pyrolytic graphite has an extremely high melting point. It is refractory and changes state at a temperature of 3650 °C as compared to copper’s melting point of just 1080 °C. Highly oriented pyrolytic graphite is thus grown on a graphite substrate in reactor vessels at temperatures of up to 3000 °C, and contaminants are simply precipitated out, resulting in an extremely pure finished product.

Highly oriented pyrolytic graphite also exhibits a very low ion erosion rate compared to copper or molybdenum [37]. For microwave devices that exhibit failure modes due to ion erosion, highly oriented pyrolytic graphite dramatically improves operational lifetime [38]. Highly oriented pyrolytic graphite also exhibits a very low vapor pressure, which reduces electron ionization of the residual gas in vacuum electron devices [39]. It is likely that gas ionization, ionization of sputtered elements, and secondary electron yield are responsible for presenting charge that is out of favorable phase to the output electrodes of vacuum devices, resulting in degraded operation [40]. In particular, this out-of-favorable-phase charge collected at the output electrodes manifests as spurious radio frequency output noise. Electrodes made from highly oriented pyrolytic graphite will thus result in vacuum devices that exhibit lower radio frequency noise at comparable operating conditions when compared with standard devices employing copper or molybdenum electrodes. Highly oriented pyrolytic graphite also possesses a very high thermal conductivity close to that of diamond and at least four times greater than that of copper. This enables highly oriented pyrolytic graphite components to dissipate far higher thermal loads before exhibiting thermal damage. This enables vacuum electron devices to be designed for and to operate at much higher power densities. Nichrome wire exhibits a thermal expansion coefficient different enough from copper and steel to ensure that the assembly is maintained under pressure even when the assembly is brought to braze temperature. The pressure applied by the fixture forces the braze alloy through the gaps between the pyrolytic graphite and the copper and effectively eliminates voids. When excess alloy is allowed to contact the fixture, it invariably bonds to the fixture. Highly oriented pyrolytic graphite is a highly pure and ordered form of synthetic graphite.

3. Results and discussion

The steady-state temperature profiles along the length of the monolayer graphene nanoribbon are presented in Figure 3 with substantially smooth edges. Graphene nanoribbons, as defined herein, refer to, for example, single or multiple layers of graphene that have an aspect ratio of greater than about 5, based on their length and their width. Graphene nanoribbons may be prepared in either oxidized or reduced forms. When not otherwise specified herein, the term graphene nanoribbons should be interpreted to encompass both oxidized graphene nanoribbons and reduced graphene nanoribbons. Longitudinally opening, as defined herein, refers to, for example, opening of carbon nanotubes along their longitudinal axis to form graphene nanoribbons. Such longitudinal opening may be thought of as an unzipping reaction of the carbon nanotubes. Narrow graphene nanoribbons, as defined herein, refers to, for example, graphene nanoribbons having widths less than about 10 nanometers. Wide graphene nanoribbons, as defined herein, refers to, for example, graphene nanoribbons having widths greater than about 10 nanometers. In some cases, wide graphene nanoribbons have widths greater than about 100 nanometers. The graphene nanoribbon has transverse edges that have a so-called armchair configuration. The longitudinal edges of the graphene nanoribbon have a perfect zigzag configuration. The nanoribbon length is assumed to be 40 nanometers. The temperature has a nonlinear dependence on the distance from the given reference point in the direction of heat flow. More specifically, in the vicinity of the hot and cold regions, there exists a nonlinear dependence of the temperature with respect to the distance. This nonlinear dependence is caused by the finite-size effect arising from the graphene nanoribbon, given the fact that the characteristic length scale of the monolayer graphene nanoribbon is much smaller than the mean free path of phonons in graphene. The mean free path of phonons in the graphene nanoribbon can vary depending on the exact structure and dimensions of the monolayer graphene nanoribbon. For example, the mean free path of phonons in graphene can be up to 700 nanometers at room temperature. As a result, the resulting temperature gradient is very steep in the vicinity of the hot and cold regions so that Fourier’s law is no longer applicable to the monolayer graphene nanoribbon. This indicates that phonon transport within the monolayer graphene nanoribbon is not fully diffusive, and the thermal

transport within the monolayer graphene nanoribbon is dominated by the mechanism of diffusive-ballistic heat conduction. In the regions between the hot slab and the cold slabs, the temperature has a more or less linear dependence on the distance, and thus the thermal conductivity can be determined by the temperature gradient.

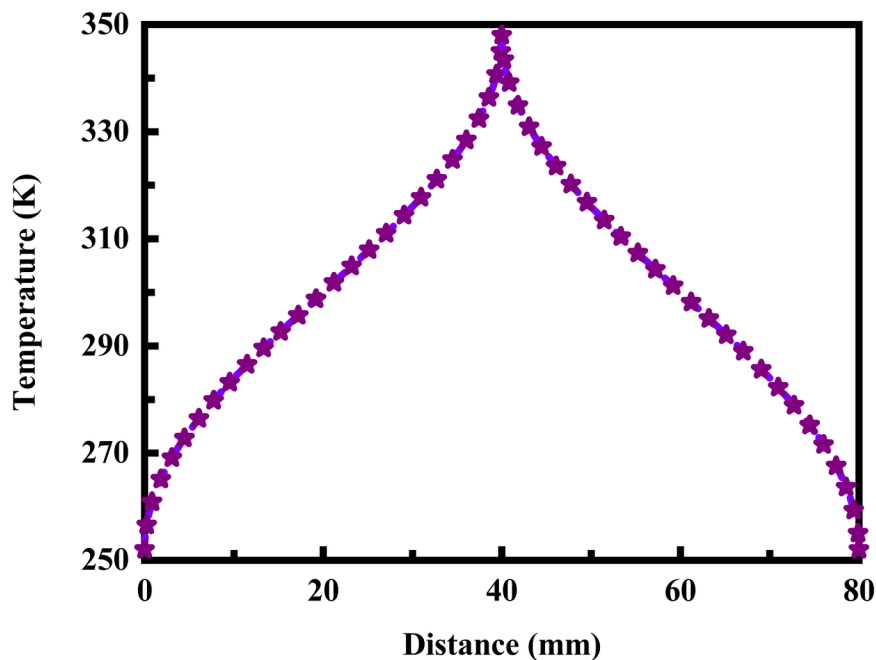


Figure 3. Steady-state temperature profiles along the length of the monolayer graphene nanoribbon with substantially smooth edges.

The thermal properties of the graphene nanoribbon with different lengths are investigated to determine the structure factors limiting the heat transfer process. The thermal conductivity can conveniently be determined by the temperature gradient in the direction of heat flow. The effect of nanoribbon length on the thermal conductivity of the monolayer graphene nanoribbon is illustrated in Figure 4 with different transverse edge termination states. The results obtained for both zigzag edges and armchair edges are presented. Shortened graphene nanoribbons, as defined herein, refers to, for example, graphene nanoribbons that have had their aspect ratios reduced by a cutting technique through their long axis. When not otherwise specified herein, the term shortened graphene nanoribbons should be interpreted to encompass both oxidized graphene nanoribbons and reduced graphene nanoribbons that have been shortened by cutting. Non-limiting means through which cutting can occur include, for example, mechanically, through application of high shear forces, through high-energy sonication, or chemically. In some cases, shortened graphene nanoribbons have aspect ratios of less than about 5. In other cases, shortened graphene nanoribbons have aspect ratios of less than about 3, or less than about 2. According to theoretical predictions, single-atomic and multiple-atomic layer graphene nanoribbons have a high surface energy that is thought to prevent their growth directly from the gas phase, even with proper nucleation. The failure to grow graphene nanoribbons directly from the gas phase is thought to be due to their tendency either to stack into graphite crystals or to fold into carbon nanotubes or similar closed structures. Although a strain energy barrier results from the curvature of the carbon nanotubes, the strain energy of the carbon nanotubes is less than the surface energy of the graphene sheets. Hence, carbon nanotubes are a preferred gas phase reaction product. The transverse edges of the graphene nanoribbon are substantially smooth. The edge termination state has little effect on the thermal conductivity, since there is little difference in thermal conductivity between zigzag-edged and armchair-edged graphene nanoribbons. However, the thermal conductivity depends strongly upon the nanoribbon length.

More specifically, the thermal conductivity increases with increasing nanoribbon length due to the reduced probability of phonon scattering from grain boundaries. This is because the mean free path of phonons in graphene, which can be up to 700 nanometers at room temperature as noted above, is very large compared to the dimensions of the graphene nanoribbon. As a result, the length of the graphene nanoribbon is vital in determining the thermal conductivity. Consequently, the length of the graphene nanoribbon is an important factor affecting the thermal properties, and must be taken into account so as to provide more accurate predictions about the thermal conductivity.

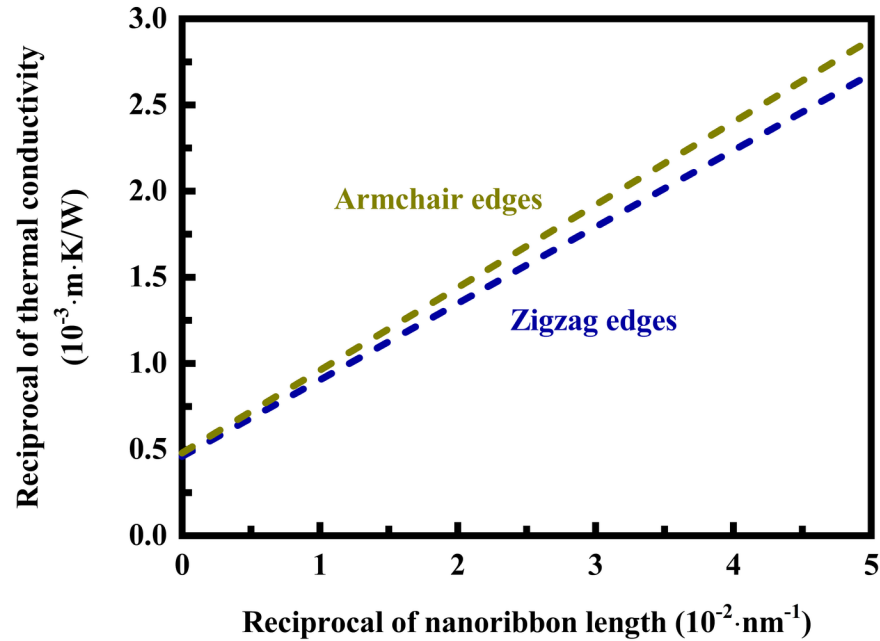


Figure 4. Effect of nanoribbon length on the thermal conductivity of the monolayer graphene nanoribbon with different transverse edge termination states.

The low-resolution scanning electron micrographs of the graphene nanoribbons are illustrated in Figure 5 for research purposes of thermal transport characteristics. The graphene nanoribbons have aspect ratios of at least 5 and the average aspect ratio of the graphene nanoribbons in the plurality of nanoribbons is at least 10 and, in some cases, at least 20. The graphene nanoribbons comprise two edges that run substantially parallel along the length of the nanoribbon and they have the armchair crystallographic direction of graphene running parallel to the nanoribbon edges. They have carbon-carbon bonds running parallel to the long nanoribbon axis. Because the graphene nanoribbons are grown, rather than patterned lithographically from graphene sheets, they are formed with atomically smooth edges. The degree of edge smoothness can be characterized by the average root mean square roughness of the edges of the nanoribbons in the array. The rms edge roughness along the length of a nanoribbon can be measured using scanning tunneling microscopy. The average rms edge roughness for the nanoribbons in a nanoribbon array will vary since longer nanoribbons within the array will tend to have rougher edges. Graphene nanoribbons outperform conventional materials and lead to next-generation technologies. Graphene nanoribbons offer tremendous promise for providing enhanced thermal transport performance. However, the full potential of graphene nanoribbons in such applications has not been realized. A major challenge facing graphene nanoribbon-based devices is that scalable approaches to create high-quality graphene nanoribbons with atomically-smooth edges are lacking. Conventional, top-down techniques in which graphene nanoribbons are etched from continuous graphene sheets result in structures with rough, disordered edges that are riddled with defects, which significantly degrade graphene's exceptional properties. This blunt top-down etching can be avoided by synthesizing

nanoribbons from the bottom-up. For instance, organic synthesis can yield ribbons with smooth edges, defined widths, and complex architectures. However, organic synthesis forms short nanoribbons and is not adapted to technologically relevant substrates, such as insulators or semiconductors, limiting its potential for commercial development. Optionally, nucleation sites can be introduced into or onto the germanium growth surface in order to control the locations at which graphene nanoribbon growth originates and the time at which graphene nanoribbon growth begins.

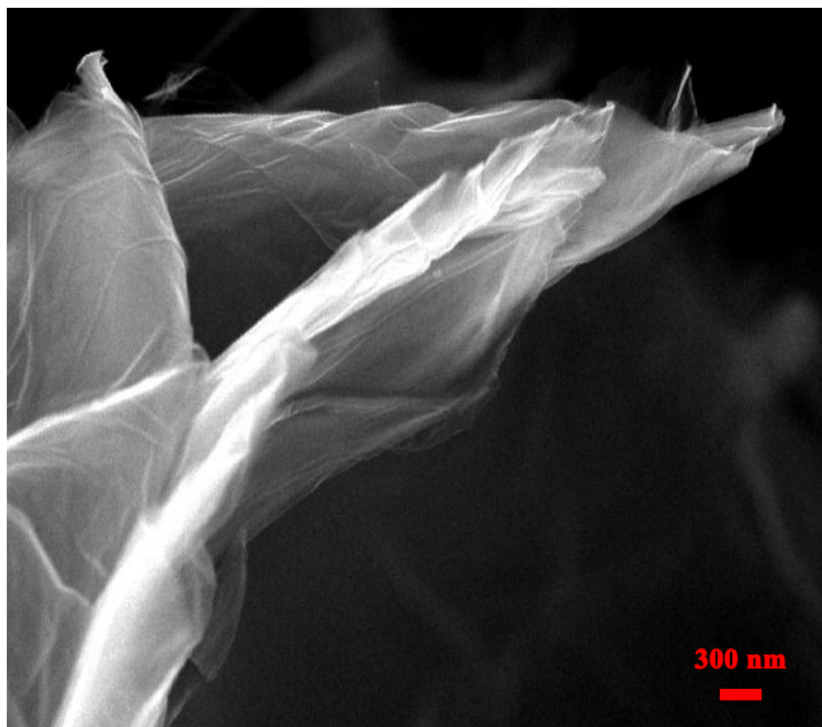


Figure 5. Low-resolution scanning electron micrographs of the graphene nanoribbons for research purposes of thermal transport characteristics.

The high-resolution scanning electron micrographs of the graphene nanoribbons are illustrated in Figure 6 for research purposes of thermal transport characteristics. The methods for preparing graphene nanoribbons described herein take place either in a liquid medium or on a surface. Without being bound by theory or mechanism, it is thought that when a free-standing graphene sheet is in solution, the excess surface energy may be stabilized by solvation energy such that folding into a carbon nanotube becomes energetically unfavorable. As a result of the solvation energy, the reverse process of longitudinally opening a carbon nanotube into a graphene nanoribbon becomes energetically favorable in an appropriate liquid medium. According to current understanding, the oxidative longitudinal opening of carbon nanotubes appears to occur along a line to afford predominantly straight-edged oxidized graphene nanoribbons. Graphene nanoribbons may be incorporated into organic and inorganic matrices such as, for example, polymer matrices. The polymer matrices can include, without limitation, thermoplastic and thermosetting polymer matrices. Incorporation of graphene nanoribbons may improve mechanical properties of the polymer composites. In some cases, polymer membranes including graphene nanoribbons may be prepared which are useful for fluid separations, antistatic applications, or electromagnetic shielding materials. The graphene nanoribbons may be dispersed as individuals in the polymer matrices. The graphene nanoribbons may also be aggregated together in two or more layers in the polymer matrices. The graphene nanoribbons may be covalently bonded to

the polymer matrices. For example, carboxylic acid groups of graphene nanoribbons may be utilized for making cross-linked polymer composites in which the graphene nanoribbons are covalently bonded to the polymer matrix. Other functional groups in the graphene nanoribbons may be utilized as well for making cross-linked polymer composites. In other cases, the graphene nanoribbons are not covalently bonded to the polymer matrices. As a non-limiting example of composite materials, reinforced rubber composites including graphene nanoribbons may be used to manufacture gaskets and seals with improved tolerance to explosive decompression. The graphene nanoribbons can be deposited from a mixture of methane gas and hydrogen gas. By varying the composition of the precursor gas mixture during growth, the duration of the growth time, and the growth temperature, the graphene nanoribbon width, length, and aspect ratio can be controlled. This control over the nanoribbon structure makes it possible to tune the graphene properties. For example, graphene undergoes a metallic-to-semiconducting transition as the nanoribbon width decreases, wherein the induced bandgap is inversely proportional to the nanoribbon width. Therefore, the present approach makes it possible to control the width of the nanoribbons and, therefore, to tailor their electronic structure. By tuning the precursor composition and growth time, nanoribbons with widths below the current lithography resolution can be achieved. Key parameters for realizing anisotropic growth are the mole fractions of the precursor molecules and the carrier molecules used in the chemical vapor deposition gas mixture, where the mole fractions can be adjusted by adjusting the partial pressures of the precursor and carrier gases. However, these parameters are not independent, so the optimum value for one of the parameters will depend on the others. The growth time also plays a role in determining the dimensions of the chemical vapor deposition-grown graphene nanoribbons. Generally, as growth time is decreased, narrower, shorter nanoribbons are formed. Therefore, by tuning the duration of the growth time and the ratio of precursor gas to carrier gas in the gas mixture, nanoribbons with desired lengths and widths can be selectively grown using bottom-up chemical vapor deposition growth. The optimum conditions for achieving anisotropic graphene growth may vary somewhat depending upon the laboratory conditions. For example, in a cleaner environment, the growth rate at a given set of conditions would be expected to be slower than in a dirtier environment. Therefore, to achieve the same low growth rate observed under standard laboratory conditions in a cleaner system, such as a clean room, a higher methane mole fraction and a lower hydrogen mole fraction could be used.

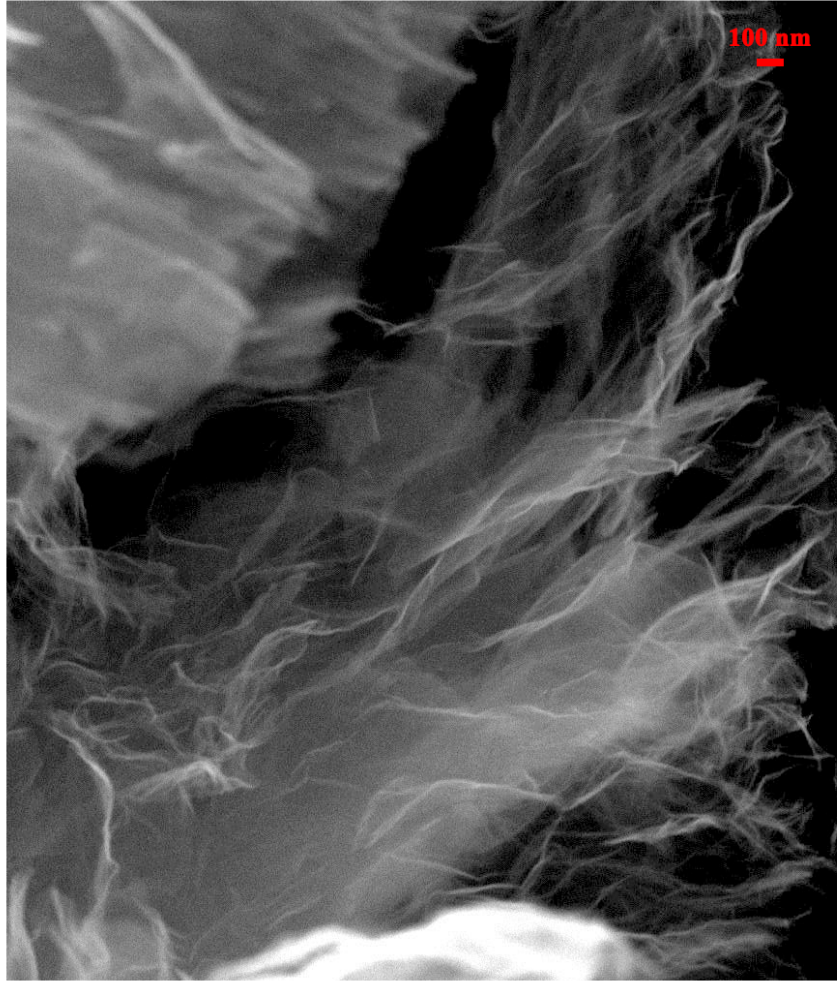


Figure 6. High-resolution scanning electron micrographs of the graphene nanoribbons for research purposes of thermal transport characteristics.

The effect of temperature on the thermal conductivity of the monolayer graphene nanoribbon is illustrated in Figure 7 with different transverse edge termination states. Graphene is a two-dimensional carbon allotrope, the electronic, and magnetic properties of which can be tuned by engineering two-dimensional graphene sheets into one-dimensional structures with confined width, known as graphene nanoribbons. The properties of graphene nanoribbons are highly dependent on their width and edge structure. Graphene nanoribbons possess a number of useful properties, including, for example, beneficial electrical properties. Unlike carbon nanotubes, which can be metallic, semi-metallic or semiconducting depending on their chiral geometry and diameter, the electrical properties of graphene nanoribbons are governed by their width and their edge configurations and functionalization. For example, graphene nanoribbons of less than about 10 nanometers in width are semiconductors, whereas similar graphene nanoribbons having a width greater than about 10 nanometers are metallic or semi-metallic conductors. The edge configurations of graphene nanoribbons having an armchair or zigzag arrangement of carbon atoms, along with the terminal edge functional groups, are also calculated to affect the transmission of electron carriers. Such armchair and zigzag arrangements are analogous to those defined in carbon nanotubes. In addition to the electrical properties, graphene nanoribbons maintain many of the desirable mechanical properties that carbon nanotubes and graphene sheets also possess. Various methods for making graphene sheets are known, including, for example, adhesive tape

exfoliation of individual graphene layers from graphite, chemical-based exfoliation of graphene layers from graphite, and chemical vapor deposition processes, each process providing on the order of picogram quantities of graphene [41, 42]. Several lithographic and synthetic procedures have been developed for producing minuscule amounts of graphene nanoribbons [43, 44]. Microscopic quantities of graphene nanoribbons have been produced by partial encapsulation of carbon nanotubes in a polymer, followed by plasma etching to longitudinally cut the carbon nanotubes [45, 46]. Macroscopic quantities of graphene nanoribbons have also been produced by a chemical vapor deposition process [47, 48]. Graphene represents an atomically thin layer of carbon in which the carbon atoms reside at regular two-dimensional lattice positions within a single sheet or a few stacked sheets of fused six-membered carbon rings. In its various forms, this material has garnered widespread interest for use in a number of applications, primarily due to its favorable combination of high electrical and thermal conductivity values, good mechanical strength, and unique electronic properties. However, an advantage of graphene over carbon nanotubes is that graphene can generally be produced in bulk much more inexpensively than can the latter, thereby addressing perceived supply and cost issues that have been commonly associated with carbon nanotubes. Despite the fact that graphene is generally synthesized more easily than are carbon nanotubes, there remain issues with production of graphene in quantities sufficient to support various commercial operations. Scalability to produce large area graphene films represents a particular problem. The most scalable processes developed to date for making graphene films utilize chemical vapor deposition technology. Graphene nanoribbons prepared by these processes are typically characterized by multiple graphene layers with a kinked morphology and irregular atomic structure. Graphene nanoribbons are a single or a few layers of the well-known carbon allotrope graphitic carbon, which possesses exceptional electrical and physical properties which may lead to various applications. Graphene nanoribbons structurally have high aspect ratio with length being much longer than the width or thickness. Graphene nanoplatelets are similar to graphene nanoribbons except that that the length is in the micron or sub-micron range and hence graphene nanoplatelets lack the high aspect ratio of graphene nanoribbons. Graphene nanoplatelets also possess many of the useful properties of carbon nanotubes and graphene nanoribbons. Graphene nanoribbons are prepared by chemical vapor deposition and from graphite using chemical processes. Most typically, graphene nanoribbons are prepared from carbon nanotubes by chemical unzipping and the quality of graphene nanoribbons depends the purity of the carbon nanotube starting material.

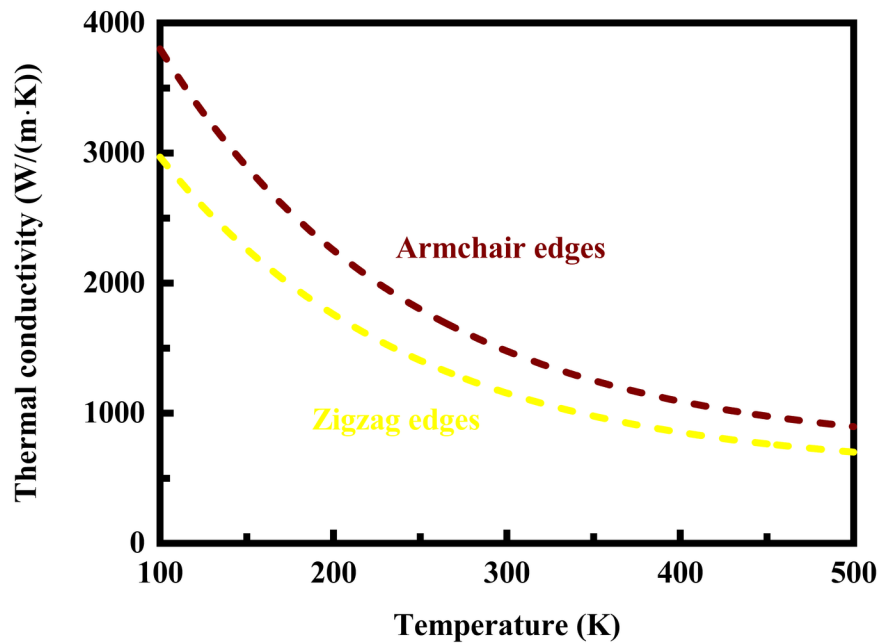


Figure 7. Effect of temperature on the thermal conductivity of the monolayer graphene nanoribbon with different transverse edge termination states.

The effect of the number of layers on the thermal conductivity of the monolayer graphene nanoribbon is illustrated in Figure 8 with different transverse edge termination states. Graphene typically refers to a material having less than about 10 graphitic layers. The graphitic layers are characterized by an infinite two-dimensional basal plane having a hexagonal lattice structure and various edge functionalities, which may include, for example, carboxylic acid groups, hydroxyl groups, epoxide groups and ketone groups. Graphene nanoribbons are a special class of graphene, which are similarly characterized by a two-dimensional basal plane, but with a large aspect ratio of their length to their width. In this regard, graphene nanoribbons bear similarity to carbon nanotubes, which have a comparable large aspect ratio defined by one or more layers of graphene sheets rolled up to form a cylinder. The graphene nanoribbons can include various layers. For instance, the graphene nanoribbons may include a single layer. In some cases, the graphene nanoribbons may include a plurality of layers. In some cases, the graphene nanoribbons include from about one layer to about eight layers. In some cases, the graphene nanoribbons include from about second layers to about ten layers. In some cases, the graphene nanoribbon layers have interlayer spacings of more than about 0.2 nanometers. In some cases, the graphene nanoribbon layers have interlayer spacings of 0.34 nanometers or larger. The graphene nanoribbons may be derived from various carbon sources. For instance, the graphene nanoribbons may be derived from carbon nanotubes, such as multi-walled carbon nanotubes. In some cases, the graphene nanoribbons are derived through the longitudinal splitting of carbon nanotubes. Various methods may be used to split carbon nanotubes to form graphene nanoribbons. Carbon nanotubes may be split by exposure to potassium, sodium, lithium, alloys thereof, metals thereof, salts thereof, and combinations thereof. For instance, the splitting may occur by exposure of the carbon nanotubes to a mixture of sodium and potassium alloys, a mixture of potassium and naphthalene solutions, and combinations thereof. In some cases, the graphene nanoribbons are made by the longitudinal splitting of carbon nanotubes using oxidizing agents or by the longitudinal opening of carbon nanotubes. The thermally conductive materials may also utilize various graphene nanoribbons. For instance, the graphene nanoribbons include, without limitation, functionalized graphene nanoribbons, pristine graphene nanoribbons, doped graphene nanoribbons, graphene oxide nanoribbons, reduced graphene oxide nanoribbons, reduced graphene oxide flakes, and combinations thereof.

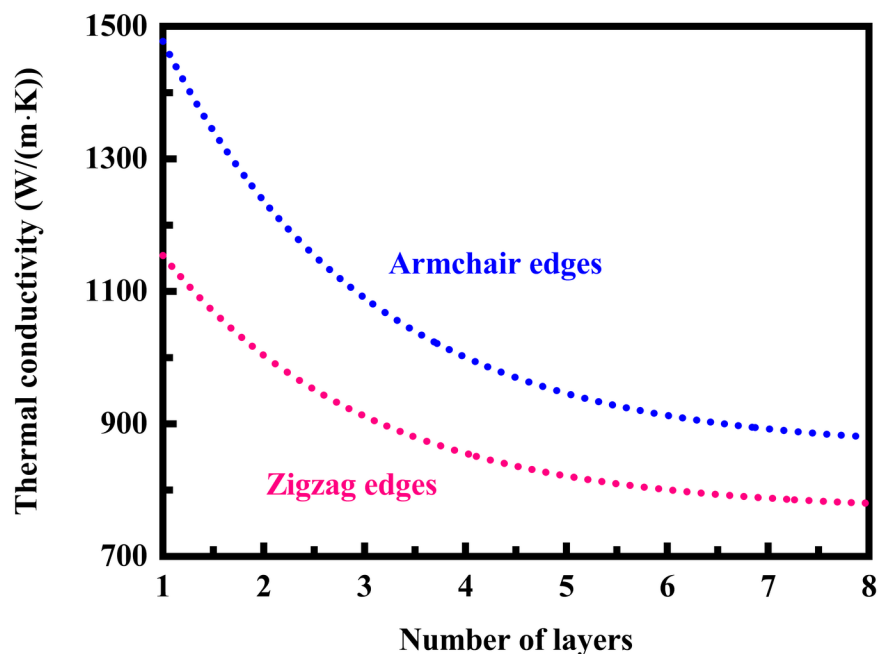


Figure 8. Effect of the number of layers on the thermal conductivity of the monolayer graphene nanoribbon with different transverse edge termination states.

4. Conclusions

The present study is focused primarily upon the thermal transport characteristics of graphene nanoribbons. The thermal transport characteristics of graphene nanoribbons are studied using molecular dynamics simulations and by experimental measurements. A specific heat flux is imposed through the graphene nanoribbon. The graphene nanoribbon is considered as a single layer of carbon atoms with each atom bound to three neighbors in a honeycomb structure. The thermal conductivity is determined from the temperature gradient obtained and the heat flux imposed. The thermal properties of the graphene nanoribbon with different lengths are investigated to determine the structure factors limiting the heat transfer process. The present study aims to provide a fundamental understanding of the thermal transport properties of graphene nanoribbons. Particular emphasis is placed upon the effect of various factors on the thermal conductivity of graphene nanoribbons under different conditions. The major conclusions are summarized as follows:

- The mean free path of phonons depends on the nanoribbon structure and dimensions.
- The thermal conductivity increases with increasing nanoribbon length.
- Graphene nanoribbons offer tremendous promise for providing enhanced transport performance.
- Graphene undergoes a metallic-to-semiconducting transition as the nanoribbon width decreases.
- The properties of graphene nanoribbons are highly dependent on their width and edge structure.
- The graphene nanoribbons can be derived through the longitudinal splitting of carbon nanotubes.

References

1. J.M. Carlsson and M. Scheffler. Structural, electronic, and chemical properties of nanoporous carbon. *Physical Review Letters* , Volume 96, Issue 4, 2006, Article Number: 046806.
2. T.O. Wehling, E. Şaşıoğlu, C. Friedrich, A.I. Lichtenstein, M.I. Katsnelson, and S. Blügel. Strength of effective coulomb interactions in graphene and graphite. *Physical Review Letters* , Volume 106, Issue 23, 2011, Article Number: 236805.
3. R.E. Smalley. Discovering the fullerenes. *Reviews of Modern Physics* , Volume 69, Issue 3, 1997, Pages 723-730.
4. P. Ayala, R. Arenal, A. Loiseau, A. Rubio, and T. Pichler. The physical and chemical properties of heteronanotubes. *Reviews of Modern Physics* , Volume 82, Issue 2, 2010, Pages 1843-1885.
5. A.M. Marconnet, M.A. Panzer, and K.E. Goodson. Thermal conduction phenomena in carbon nanotubes and related nanostructured materials. *Reviews of Modern Physics* , Volume 85, Issue 3, 2013, Pages 1295-1326.
6. K.L. Klein, A.V. Melechko, T.E. McKnight, S.T. Retterer, P.D. Rack, J.D. Fowlkes, D.C. Joy, and M.L. Simpson. Surface characterization and functionalization of carbon nanofibers. *Journal of Applied Physics* , Volume 103, Issue 6, 2008, Article Number: 061301.
7. S. Mrozowski. Zone structure of graphite. *Physical Review* , Volume 92, Issue 5, 1953, Pages 1320-1321.
8. J.C. Slonczewski and P.R. Weiss. Band structure of graphite. *Physical Review* , Volume 109, Issue 2, 1958, Pages 272-279.
9. H. Shioyama. The interactions of two chemical species in the interlayer spacing of graphite. *Synthetic Metals* , Volume 114, Issue 1, 2000, Pages 1-15.
10. C. Binns, S.H. Baker, C. Demangeat, and J.C. Parlebas. Growth, electronic, magnetic and spectroscopic properties of transition metals on graphite. *Surface Science Reports* , Volume 34, Issues 4-5, 1999, Pages 107-170.
11. P.M. Adams, H.A. Katzman, G.S. Rellick, and G.W. Stupian. Characterization of high thermal conductivity carbon fibers and a self-reinforced graphite panel. *Carbon* , Volume 36, Issue 3, 1998, Pages 233-245.
12. M. Kerford and R.P. Webb. An investigation of the thermal profiles induced by energetic carbon molecules on a graphite surface. *Carbon* , Volume 37, Issue 5, 1999, Pages 859-864.
13. R.S. Rubino and E.S. Takeuchi. The study of irreversible capacity in lithium-ion anodes prepared with

- thermally oxidized graphite. *Journal of Power Sources* , Volumes 81-82, 1999, Pages 373-377.
14. J. Gibkes, B.K. Bein, D. Krüger, and J. Pelzl. Thermophysical characterization of fine-grain graphites based on thermal waves. *Carbon* , Volume 31, Issue 5, 1993, Pages 801-807.
 15. P.G. Klemens and D.F. Pedraza. Thermal conductivity of graphite in the basal plane. *Carbon* , Volume 32, Issue 4, 1994, Pages 735-741.
 16. M.S. Seehra and A.S. Pavlovic. X-Ray diffraction, thermal expansion, electrical conductivity, and optical microscopy studies of coal-based graphites. *Carbon* , Volume 31, Issue 4, 1993, Pages 557-564.
 17. D. Angermeier, R. Monna, A. Slaoui, and J.C. Muller. Analysis of thin film polysilicon on graphite substrates deposited in a thermal CVD system. *Journal of Crystal Growth* , Volume 191, Issue 3, 1998, Pages 386-392.
 18. C.-C. Hung and J. Miller. Thermal conductivity of pristine and brominated highly graphitized pitch based carbon fibers. *Carbon* , Volume 25, Issue 5, 1987, Pages 679-684.
 19. B. Kastelein, R.D.V. Bergen, H. Postma, H.C. Meijer, and F. Mathu. Thermal conductance of highly oriented pyrolytic graphite along the c-direction at very low temperatures including magnetic field effects. *Carbon* , Volume 30, Issue 6, 1992, Pages 845-850.
 20. B.T. Kelly and K.E. Gilchrist. The basal thermal conductivity of highly oriented pyrolytic graphite as a function of degree of graphitization. *Carbon* , Volume 7, Issue 3, 1969, Pages 355-358.
 21. V.J. Cee, D.L. Patrick, and T.P. Beebe. Unusual aspects of superperiodic features on highly oriented pyrolytic graphite. *Surface Science* , Volume 329, Issues 1-2, 1995, Pages 141-148.
 22. F. Rodriguez-reinoso and P.A. Thrower. Microscopic studies of oxidized highly oriented pyrolytic graphites. *Carbon* , Volume 12, Issue 3, 1974, Pages 269-279.
 23. J. Kim, D. Kim, K.W. Lee, E.H. Choi, S.J. Noh, H.S. Kim, and C.E. Lee. Proton-irradiation effects on the charge transport in highly oriented pyrolytic graphite. *Solid State Communications* , Volume 186, 2014, Pages 5-7.
 24. H. Fredriksson, D. Chakarov, and B. Kasemo. Patterning of highly oriented pyrolytic graphite and glassy carbon surfaces by nanolithography and oxygen plasma etching. *Carbon* , Volume 47, Issue 5, 2009, Pages 1335-1342.
 25. T. Scheike, P. Esquinazi, A. Setzer, and W. Böhlmann. Granular superconductivity at room temperature in bulk highly oriented pyrolytic graphite samples. *Carbon* , Volume 59, 2013, Pages 140-149.
 26. D. Díaz-Fernández, J. Méndez, A.D. Campo, R.J.O. Mossaneck, M. Abbate, M.A. Rodríguez, G. Domínguez-Cañizares, O. Bomati-Miguel, A. Gutiérrez, and L. Soriano. Nanopatterning on highly oriented pyrolytic graphite surfaces promoted by cobalt oxides. *Carbon* , Volume 85, 2015, Pages 89-98.
 27. M.D. Shirk and P.A. Molian. Ultra-short pulsed laser ablation of highly oriented pyrolytic graphite. *Carbon* , Volume 39, Issue 8, 2001, Pages 1183-1193.
 28. J. Humlíček, A. Nebojsa, F. Munz, M. Miric, and R. Gajic. Infrared ellipsometry of highly oriented pyrolytic graphite. *Thin Solid Films* , Volume 519, Issue 9, 2011, Pages 2624-2626.
 29. E. Pollmann, P. Ernst, L. Madauß, and M. Schleberger. Ion-mediated growth of ultra thin molybdenum disulfide layers on highly oriented pyrolytic graphite. *Surface and Coatings Technology* , Volume 349, 2018, Pages 783-786.
 30. Z.-H. Wang, K. Kanai, K. Iketaki, Y. Ouchi, and K. Seki. Epitaxial growth of p-sexiphenyl film on highly oriented pyrolytic graphite surface studied by scanning tunneling microscopy. *Thin Solid Films* , Volume 516, Issue 9, 2008, Pages 2711-2715.
 31. N. Bajales, M. Ávila, V. Galván, and P.G. Bercoff. Multi-characterization of electron-induced defects in highly oriented pyrolytic graphite. *Current Applied Physics* , Volume 16, Issue 3, 2016, Pages 421-427.
 32. D.S. Martin, P. Weightman, and J.T. Gauntlett. The adsorption of n-hexadecane onto highly oriented pyrolytic graphite studied by atomic force microscopy. *Surface Science* , Volume 398, Issue 3, 1998, Pages 308-317.
 33. A.M. Borisov, E.S. Mashkova, A.S. Nemov, and E.S. Parilis. Effect of radiation damage on ion-induced electron emission from highly oriented pyrolytic graphite. *Vacuum* , Volume 80, Issue 4, 2005, Pages 295-301.

34. M.A. Mannan, H. Noguchi, T. Kida, M. Nagano, N. Hirao, and Y. Baba. Growth and characterization of stoichiometric BCN films on highly oriented pyrolytic graphite by radiofrequency plasma enhanced chemical vapor deposition. *Thin Solid Films* , Volume 518, Issue 15, 2010, Pages 4163-4169.
35. D.S. Martin, P. Weightman, and J.T. Gauntlett. The evaporation of n-hexadecane from highly oriented pyrolytic graphite studied by atomic force microscopy. *Surface Science* , Volume 417, Issues 2-3, 1998, Pages 390-405.
36. Y. Baba, K. Nagata, S. Takahashi, N. Nakamura, N. Yoshiyasu, M. Sakurai, C. Yamada, S. Ohtani, and M. Tona. Surface modification on highly oriented pyrolytic graphite by slow highly charged ions. *Surface Science* , Volume 599, Issues 1-3, 2005, Pages 248-254.
37. R.S. Holt. Electron correlation effects in the momentum distribution of highly oriented pyrolytic graphite. *Solid State Communications* , Volume 59, Issue 5, 1986, Pages 321-323.
38. D.-Q. Yang, K.N. Piyakis, and E. Sacher. The manipulation of Cu cluster dimensions on highly oriented pyrolytic graphite surfaces by low energy ion beam irradiation. *Surface Science* , Volume 536, Issues 1-3, 2003, Pages 67-74.
39. E. Vetrivendan, R. Hareesh, and S. Ningshen. Synthesis and characterization of chemical vapour deposited pyrolytic graphite. *Thin Solid Films* , Volume 749, 2022, Article Number: 139180.
40. P. Touzain and A. Hamwi. De-intercalation and second intercalation of potassium into a highly oriented pyrolytic graphite. *Synthetic Metals* , Volume 23, Issues 1-4, 1988, Pages 127-132.
41. S. Kiddell, Y. Kazemi, J. Sorken, and H. Naguib. Influence of flash graphene on the acoustic, thermal, and mechanical performance of flexible polyurethane foam. *Polymer Testing* , Volume 119, 2023, Article Number: 107919.
42. R.P. Yali, A. Mehri, and M. Jamaati. Nonlinear thermal transport in graphene nanoribbon: A molecular dynamics study. *Physica A: Statistical Mechanics and its Applications* , Volume 610, 2023, Article Number: 128416.
43. J.C. Bi, H. Yun, M. Cho, M.-G. Kwak, B.-K. Ju, and Y. Kim. Thermal conductivity and mechanical durability of graphene composite films containing polymer-filled connected multilayer graphene patterns. *Ceramics International* , Volume 48, Issue 12, 2022, Pages 17789-17794.
44. H. Yun, D.G. Yang, J.C. Bi, M.-G. Kwak, and Y. Kim. Fabrication and properties of thermally conductive adhesive tapes containing multilayer graphene patterns. *Ceramics International* , Volume 48, Issue 22, 2022, Pages 34053-34058.
45. Z. Moradi, M. Vaezzadeh, and M. Saeidi. Temperature-dependent thermal expansion of graphene. *Physica A: Statistical Mechanics and its Applications* , Volume 512, 2018, Pages 981-985.
46. H. Rezaia and M. Yarmohammadi. Dynamical thermal conductivity of bilayer graphene in the presence of bias voltage. *Physica E: Low-dimensional Systems and Nanostructures* , Volume 75, 2016, Pages 125-135.
47. K.K. Choudhary. Investigation of two-dimensional lattice thermal transport in bilayer graphene using phonon scattering mechanism. *Physica E: Low-dimensional Systems and Nanostructures* , Volume 58, 2014, Pages 106-110.
48. N. Usha, V. Subramanian, V.R.K. Murthy, and J. Sobhanadri. Microwave studies on some low stage graphite ferric chloride intercalation compound. *Materials Science and Engineering: B* , Volume 45, Issues 1-3, 1997, Pages 85-87.

Computational modelling and experimental study of the thermal transport characteristics of graphene nanoribbons

Junjie Chen

Department of Energy and Power Engineering, School of Mechanical and Power Engineering, Henan Polytechnic University, Jiaozuo, Henan, 454000, P.R. China

* Corresponding author, E-mail address: cjjtpj@163.com, <https://orcid.org/0000-0002-4222-1798>

Abstract

Graphene is a two-dimensional form of crystalline carbon, either a single layer of carbon atoms forming a hexagonal lattice or several coupled layers of this honeycomb structure. Graphene is a parent form of all graphitic structures of carbon. However, the field of graphene science and technology is relatively new. Progress depends not only on the basic science but also on the development of new ways to produce graphene on an industrial scale. The present study is focused primarily upon the thermal transport characteristics of graphene nanoribbons. The thermal transport characteristics of graphene nanoribbons are studied using molecular dynamics simulations and by experimental measurements. A specific heat flux is imposed through the graphene nanoribbon. The graphene nanoribbon is considered as a single layer of carbon atoms with each atom bound to three neighbors in a honeycomb structure. The thermal conductivity is determined from the temperature gradient obtained and the heat flux imposed. The present study aims to provide a fundamental understanding of the thermal transport properties of graphene nanoribbons. Particular emphasis is placed upon the effect of various factors on the thermal conductivity of graphene nanoribbons under different conditions. The results indicate that the mean free path of phonons depends on the nanoribbon structure and dimensions. The thermal conductivity increases with increasing nanoribbon length. Graphene nanoribbons offer tremendous promise for providing enhanced transport performance. Graphene undergoes a metallic-to-semiconducting transition as the nanoribbon width decreases. The properties of graphene nanoribbons are highly dependent on their width and edge structure. The graphene nanoribbons can be derived through the longitudinal splitting of carbon nanotubes.

Keywords: Graphene nanoribbons; Graphitic structures; Carbon nanotubes; Carbon nanofibers; Thermal properties; Thermal conductivity

1. Introduction

Elemental carbon exists in several forms, each of which has its own physical characteristics. Two of its well-defined forms, diamond and graphite, are crystalline in structure, but they differ in physical properties because the arrangements of the atoms in their structures are dissimilar. A third form, called fullerene, consists of a variety of molecules composed entirely of carbon. Spheroidal, closed-cage fullerenes are called buckminsterfullerenes, or buckyballs, and cylindrical fullerenes are called carbon nanotubes. Carbon has five unique crystalline structures, namely diamond, fullerene, carbon nanotubes or carbon nanofibers, graphene, and graphite [1, 2]. Fullerene is a zero-dimensional nano-graphitic material [3]. Carbon nanotubes and carbon nanofibers are a one-dimensional nanocarbon or nano-graphitic material [4]. Carbon nanotubes and carbon nanofibers have a diameter on the order of a few nanometers to a few hundred nanometers. Their longitudinal, hollow structures impart unique chemical, electrical, and mechanical properties to the material [5, 6]. Graphene is a two-dimensional nano-graphitic material and graphite is a three-dimensional graphitic material.

Bulk natural graphite is a three-dimensional graphitic material, and each graphite particle is composed of multiple grains with grain boundaries that demarcate adjacent graphite single crystals. Each grain is composed of multiple graphene planes that are oriented parallel to each other. A graphene plane in a graphite crystallite is composed of carbon atoms occupying a two-dimensional, hexagonal lattice [7, 8]. In a given grain or single crystal, the graphene planes are stacked and bonded through van der Waal forces in a direction perpendicular to the graphene plane. Although all the graphene planes in one grain are parallel to each other, typically the graphene planes in one grain and the graphene planes in an adjacent grain are inclined at different orientations [9, 10]. This means that the orientations of the various grains in a graphite particle typically differ from each other.

A graphite single crystal per se is anisotropic with a property measured along a direction in the basal plane being dramatically different than if measured along the crystallographic c-axis direction [11, 12]. For instance, the thermal conductivity of a graphite single crystal can be up to approximately 1,920 W/(m·K) or approximately 1,800 W/(m·K) in the basal plane [13, 14], but that along the crystallographic c-axis direction is less than approximately 10 W/(m·K) [15, 16]. Further, the multiple grains or crystallites in a graphite particle are typically all oriented along different and random directions [17, 18]. Consequently, a natural graphite particle composed of multiple grains of different orientations exhibits an average property between these two extremes.

It would be highly desirable in many applications to produce a graphitic film containing single or multiple graphene grains, having sufficiently large dimensions and having all graphene planes being essentially parallel to one another along one desired direction [19, 20]. In other words, it is highly desirable to have one large-size graphitic film having the c-axis directions of all the graphene planes being substantially parallel to one another and having a sufficiently large film length and width for a particular application [21, 22]. It has not been possible to produce such a highly oriented graphitic film [23, 24]. Even though some attempts have been made to produce the so-called highly oriented pyrolytic graphite through tedious, energy intensive, and expensive chemical vapor deposition followed by ultra-high temperature graphitization [25, 26], the graphitic structure of the highly oriented pyrolytic graphite remains inadequately aligned and laden with defects and, hence, exhibits properties that are significantly lower than what are theoretically predicted.

The constituent graphene planes of a graphite crystallite in a natural or artificial graphite particle can be exfoliated and extracted or isolated to obtain individual graphene sheets of carbon atoms provided the inter-planar van der Waals forces can be overcome [27, 28]. An isolated, individual graphene sheet of carbon atoms is commonly referred to as single-layer graphene [29, 30]. A stack of multiple graphene planes bonded through van der Waals forces in the thickness direction with an inter-graphene plane spacing of approximately 0.3354 nanometers is commonly referred to as a multi-layer graphene [31, 32]. A multi-layer graphene platelet has up to 300 layers of graphene planes, but more typically up to 30 graphene planes, even more typically up to 20 graphene planes, and most typically up to 10 graphene planes [33, 34]. Single-layer graphene and multi-layer graphene sheets are collectively called nanographene platelets [35, 36]. Graphene or graphene oxide sheets or platelets are a new class of carbon nanomaterial that is distinct from the zero-dimensional fullerene, the one-dimensional carbon nanotubes, and the three-dimensional graphite.

Graphene is a two-dimensional form of crystalline carbon, either a single layer of carbon atoms forming a hexagonal lattice or several coupled layers of this honeycomb structure. Graphene is a parent form of all graphitic structures of carbon. However, the field of graphene science and technology is relatively new. Progress depends not only on the basic science but also on the development of new ways to produce graphene on an industrial scale. The present study is focused primarily upon the thermal transport characteristics of graphene nanoribbons. The thermal transport characteristics of graphene nanoribbons are studied using molecular dynamics simulations and by experimental

measurements. A specific heat flux is imposed through the graphene nanoribbon. The graphene nanoribbon is considered as a single layer of carbon atoms with each atom bound to three neighbors in a honeycomb structure. The thermal conductivity is determined from the temperature gradient obtained and the heat flux imposed. The present study aims to provide a fundamental understanding of the thermal transport properties of graphene nanoribbons. Particular emphasis is placed upon the effect of various factors on the thermal conductivity of graphene nanoribbons under different conditions.

2. Methods

The honeycomb lattice of graphene actually consists of two sublattices, designated A and B, such that each atom in sublattice A is surrounded by three atoms of sublattice B and vice versa. This simple geometrical arrangement leads to the appearance that the electrons and holes in graphene have an unusual degree of internal freedom, usually called pseudospin. In fact, making the analogy more complete, pseudospin mimics the spin, or internal angular momentum, of subatomic particles. Within this analogy, electrons and holes in graphene play the same role as particles and antiparticles in quantum electrodynamics. This makes graphene a test bed for high-energy physics: some quantum relativistic effects that are hardly reachable in experiments with subatomic particles using particle accelerators have clear analogs in the physics of electrons and holes in graphene, which can be measured and studied more easily because of their lower velocity. Thus, graphene provides a bridge between materials science and some areas of fundamental physics.

There is another reason why graphene is of special interest to fundamental science. Graphene is the first and simplest example of a two-dimensional crystal, that is, a solid material that contains just a single layer of atoms arranged in an ordered pattern. Two-dimensional systems are of huge interest not only for physics and chemistry but also for other natural sciences. In many respects, two-dimensional systems are fundamentally different from three-dimensional systems. In particular, due to very strong thermal fluctuations of atomic positions that remain correlated at large distances, long-range crystalline order cannot exist in two dimensions. Instead, only short-range order exists, and it does so only on some finite scale of characteristic length, a caveat that should be noted when graphene is called a two-dimensional crystal. For this reason, two-dimensional systems are inherently flexural, manifesting strong bending fluctuations, so that they cannot be flat and are always rippled or corrugated. Graphene, because of its relative simplicity, can be considered as a model system for studying two-dimensional physics and chemistry in general. Other two-dimensional crystals besides graphene can be derived by exfoliation from other multilayer crystals, for example, hexagonal boron nitride, molybdenum disulfide, or tungsten disulfide, or by chemical modification of graphene, for example, hydrogenated graphene, or fluorinated graphene. Modern electronics are basically two-dimensional in that they use mainly the surface of semiconducting materials. Therefore, graphene and other two-dimensional materials are considered very promising for many such applications. Using graphene, for example, it should be possible to make electronic devices that are much thinner than devices made of traditional materials. Graphene does not have an insulator state, and conductivity remains finite at any doping.

The thermal transport characteristics of graphene nanoribbons are studied using molecular dynamics simulations. A specific heat flux imposed through the graphene nanoribbon modeled in this study is depicted schematically in Figure 1 in a shape of rectangle. The graphene nanoribbon is monolayer and thus can be considered as a single layer of carbon atoms with each atom bound to three neighbors in a honeycomb structure. The substantially flat monolayer of carbon atoms is usually referred to as the basal plane of the graphene nanoribbon. The monolayer graphene nanoribbon includes an edge irregularity, such as a zig-zag configuration edge or an armchair-configuration edge. The transverse edges at both ends of the graphene nanoribbon are rough, whereas the longitudinal edges at both sides of the graphene nanoribbon are substantially smooth. It is worth noting that the

direction of heat flow is perpendicular to the irregularly shaped edges of the graphene nanoribbon. The transverse edges at both ends of the nanostructured graphene nanoribbon are atomically-disordered in the form of roughness. This edge disorder can degrade the thermal, electronic, and structural properties of the nanostructured graphene nanoribbon, including its electron mobility and strength. The graphene nanoribbon has a generally square shape with the width approximately equal to the length. The graphene nanoribbon has a generally square shape with the width approximately equal to the length.

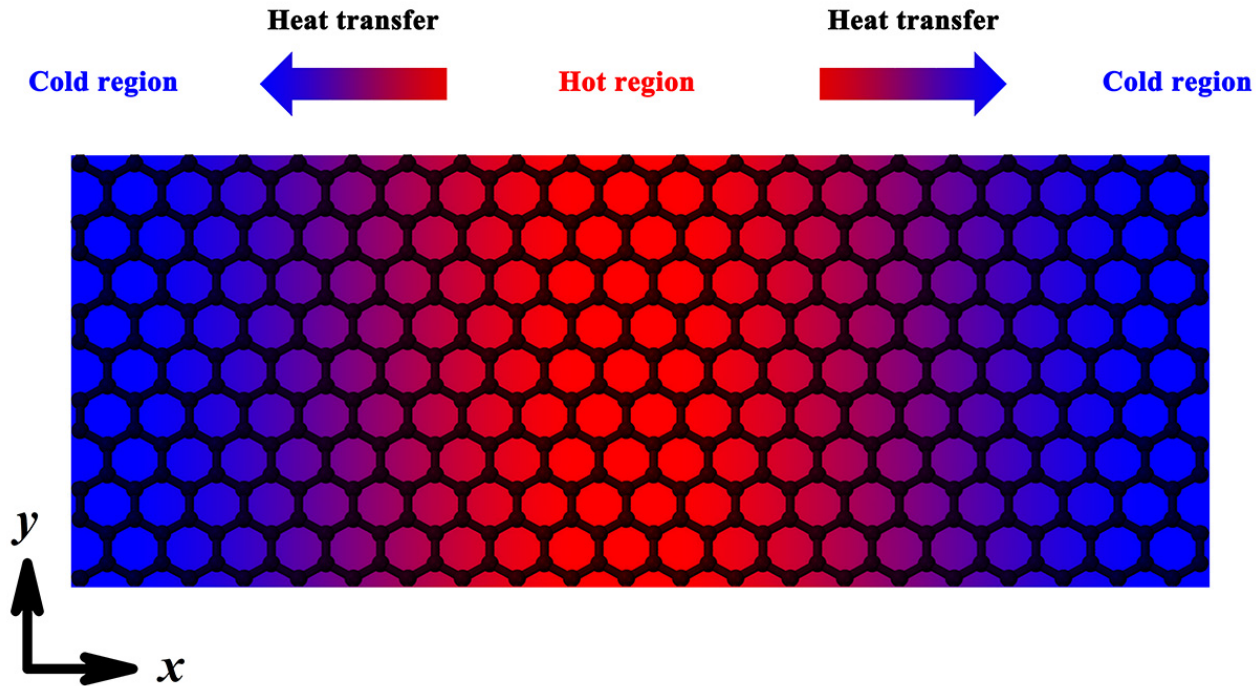


Figure 1. Schematic diagram of a specific heat flux imposed through one individual graphene nanoribbon in a shape of rectangle. It is assumed and indicated that the property being transported in the graphene nanoribbon flows from the red region to the blue regions. Linear momentum of the atoms is transferred to maintain a constant heat flux between the red region and the blue regions.

The length of the monolayer graphene nanoribbon is typically significantly greater than its width, but of course, there are exceptions. A specific heat flux imposed through the graphene nanoribbon modeled in this study is depicted schematically in Figure 2 in a shape of square. Unless otherwise stated, the graphene nanoribbon is 5.4 nanometers in width, 40 nanometers in length, and 0.335 nanometers in thickness. The structure of the graphene nanoribbon is divided into specific regions by defining hot and cold slabs. Heat is continually being transferred from the hot slab to the cold slabs so as to equalize the temperature within the graphene nanoribbon. The temperature gradient can be determined in the direction of heat flow, since the total energy is conserved in the heat conduction process. Accordingly, the thermal conductivity can be determined from the temperature gradient obtained and the heat flux imposed. The basic rate equation of the heat conduction process within the graphene nanoribbon is known as Fourier's law of heat conduction. The ratio of heat flux to the slope of the temperature profile is proportional to the thermal conductivity of the graphene nanoribbon. Fourier's Law therefore provides the definition of the thermal conductivity of the graphene nanoribbon, and forms the basis of the general method that can be used to determine its value. The thermal conductivity of the monolayer graphene nanoribbon is proportional to the effective mean free path for phonon scattering. Therefore, the thermal conductivity variation over a range of the effective mean free path for phonon scattering can be represented as a straight line. Additionally, the intrinsic thermal conductivity of the two-dimensional carbon-based material can be derived from the intercept of the straight line by extrapolation from the case with infinite length.

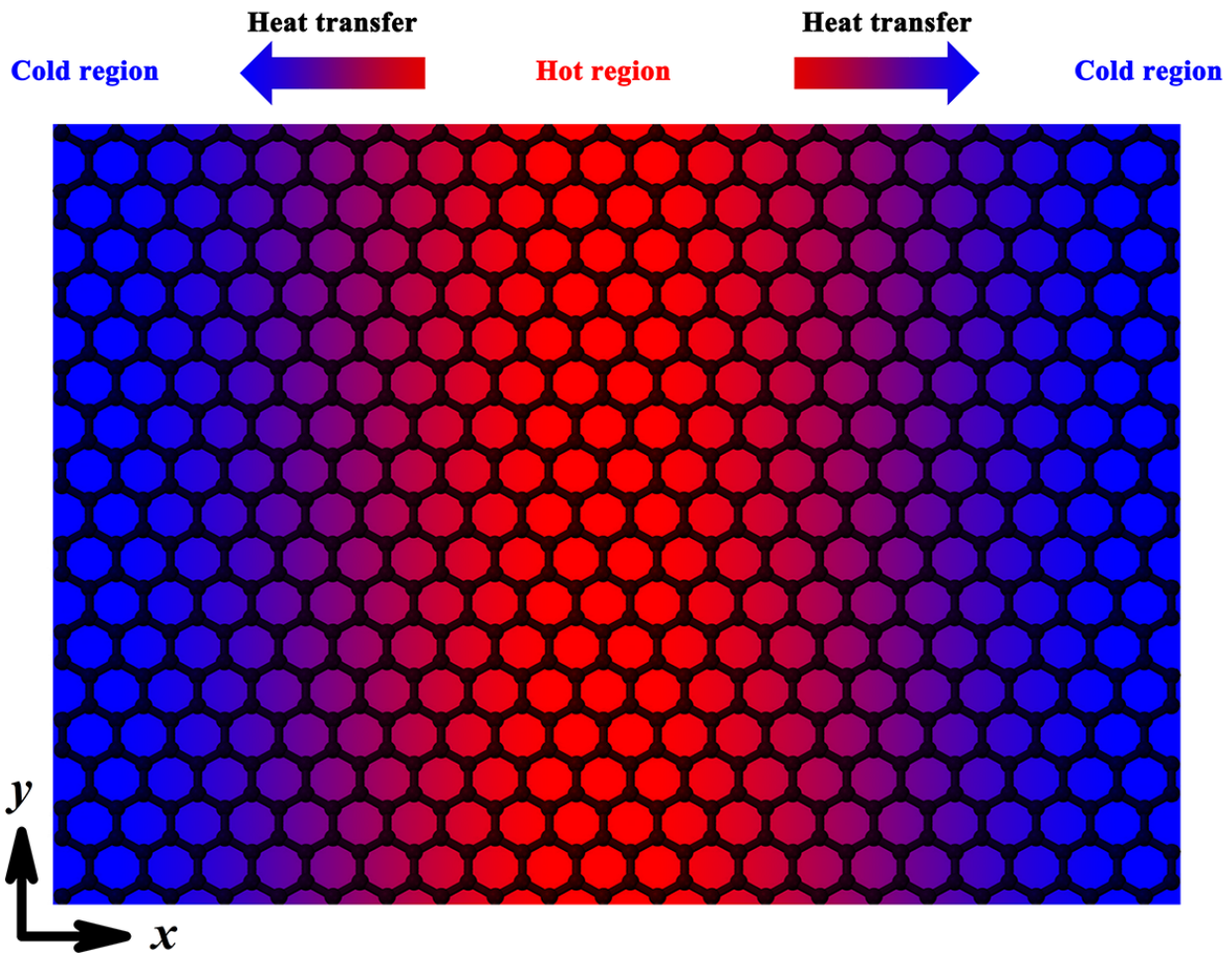


Figure 2. Schematic diagram of a specific heat flux imposed through one individual graphene nanoribbon in a shape of square. The red region has a higher value of temperature than the blue regions and that the property being transported in the graphene nanoribbon therefore flows from the red region to the blue regions. The arrows indicate the direction of heat transfer between the hot and cold regions. Linear momentum of the atoms is transferred to maintain a constant heat flux between the red region and the blue regions and a constant temperature gradient across the graphene nanoribbon.

Graphite generally comprises multiple layers of carbon atoms arranged in planar hexagonal lattices. In its highly oriented pyrolytic form, the hexagonal lattice sheets have an angular spread of less than one degree. This structure results in properties that are highly desirable for use in vacuum electron devices. For example, highly oriented pyrolytic graphite is well suited for use as a vacuum barrier. When used to manufacture components that form part of the vacuum seal, highly oriented pyrolytic graphite maintains vacuum integrity. Highly oriented pyrolytic graphite also possesses the lowest sputtering rate of all materials. Thus, electrodes made from highly oriented pyrolytic graphite will emit far fewer contaminating trace elements during operation than will copper or molybdenum electrodes. Further contributing to this property is that fact that highly oriented pyrolytic graphite has an extremely high melting point. It is refractory and changes state at a temperature of 3650 °C as compared to copper's melting point of just 1080 °C. Highly oriented pyrolytic graphite is thus grown on a graphite substrate in reactor vessels at temperatures of up to 3000 °C, and contaminants are simply precipitated out, resulting in an extremely pure finished product.

Highly oriented pyrolytic graphite also exhibits a very low ion erosion rate compared to copper or molybdenum [37]. For microwave devices that exhibit failure modes due to ion erosion, highly oriented pyrolytic graphite dramatically improves operational lifetime [38]. Highly oriented pyrolytic graphite also exhibits a very low vapor pressure, which reduces electron ionization of the residual gas in vacuum

electron devices [39]. It is likely that gas ionization, ionization of sputtered elements, and secondary electron yield are responsible for presenting charge that is out of favorable phase to the output electrodes of vacuum devices, resulting in degraded operation [40]. In particular, this out-of-favorable-phase charge collected at the output electrodes manifests as spurious radio frequency output noise. Electrodes made from highly oriented pyrolytic graphite will thus result in vacuum devices that exhibit lower radio frequency noise at comparable operating conditions when compared with standard devices employing copper or molybdenum electrodes. Highly oriented pyrolytic graphite also possesses a very high thermal conductivity close to that of diamond and at least four times greater than that of copper. This enables highly oriented pyrolytic graphite components to dissipate far higher thermal loads before exhibiting thermal damage. This enables vacuum electron devices to be designed for and to operate at much higher power densities. Nichrome wire exhibits a thermal expansion coefficient different enough from copper and steel to ensure that the assembly is maintained under pressure even when the assembly is brought to braze temperature. The pressure applied by the fixture forces the braze alloy through the gaps between the pyrolytic graphite and the copper and effectively eliminates voids. When excess alloy is allowed to contact the fixture, it invariably bonds to the fixture. Highly oriented pyrolytic graphite is a highly pure and ordered form of synthetic graphite.

3. Results and discussion

The steady-state temperature profiles along the length of the monolayer graphene nanoribbon are presented in Figure 3 with substantially smooth edges. Graphene nanoribbons, as defined herein, refer to, for example, single or multiple layers of graphene that have an aspect ratio of greater than about 5, based on their length and their width. Graphene nanoribbons may be prepared in either oxidized or reduced forms. When not otherwise specified herein, the term graphene nanoribbons should be interpreted to encompass both oxidized graphene nanoribbons and reduced graphene nanoribbons. Longitudinally opening, as defined herein, refers to, for example, opening of carbon nanotubes along their longitudinal axis to form graphene nanoribbons. Such longitudinal opening may be thought of as an unzipping reaction of the carbon nanotubes. Narrow graphene nanoribbons, as defined herein, refers to, for example, graphene nanoribbons having widths less than about 10 nanometers. Wide graphene nanoribbons, as defined herein, refers to, for example, graphene nanoribbons having widths greater than about 10 nanometers. In some cases, wide graphene nanoribbons have widths greater than about 100 nanometers. The graphene nanoribbon has transverse edges that have a so-called armchair configuration. The longitudinal edges of the graphene nanoribbon have a perfect zigzag configuration. The nanoribbon length is assumed to be 40 nanometers. The temperature has a nonlinear dependence on the distance from the given reference point in the direction of heat flow. More specifically, in the vicinity of the hot and cold regions, there exists a nonlinear dependence of the temperature with respect to the distance. This nonlinear dependence is caused by the finite-size effect arising from the graphene nanoribbon, given the fact that the characteristic length scale of the monolayer graphene nanoribbon is much smaller than the mean free path of phonons in graphene. The mean free path of phonons in the graphene nanoribbon can vary depending on the exact structure and dimensions of the monolayer graphene nanoribbon. For example, the mean free path of phonons in graphene can be up to 700 nanometers at room temperature. As a result, the resulting temperature gradient is very steep in the vicinity of the hot and cold regions so that Fourier's law is no longer applicable to the monolayer graphene nanoribbon. This indicates that phonon transport within the monolayer graphene nanoribbon is not fully diffusive, and the thermal transport within the monolayer graphene nanoribbon is dominated by the mechanism of diffusive-ballistic heat conduction. In the regions between the hot slab and the cold slabs, the temperature has a more or less linear dependence on the distance, and thus the thermal conductivity can be determined by the temperature gradient.

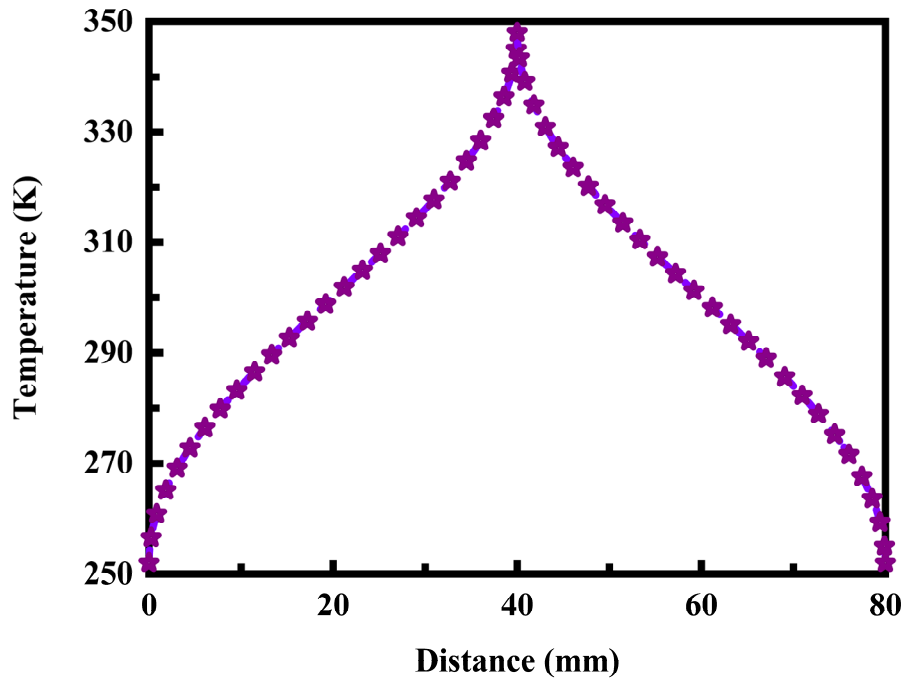


Figure 3. Steady-state temperature profiles along the length of the monolayer graphene nanoribbon with substantially smooth edges.

The thermal properties of the graphene nanoribbon with different lengths are investigated to determine the structure factors limiting the heat transfer process. The thermal conductivity can conveniently be determined by the temperature gradient in the direction of heat flow. The effect of nanoribbon length on the thermal conductivity of the monolayer graphene nanoribbon is illustrated in Figure 4 with different transverse edge termination states. The results obtained for both zigzag edges and armchair edges are presented. Shortened graphene nanoribbons, as defined herein, refers to, for example, graphene nanoribbons that have had their aspect ratios reduced by a cutting technique through their long axis. When not otherwise specified herein, the term shortened graphene nanoribbons should be interpreted to encompass both oxidized graphene nanoribbons and reduced graphene nanoribbons that have been shortened by cutting. Non-limiting means through which cutting can occur include, for example, mechanically, through application of high shear forces, through high-energy sonication, or chemically. In some cases, shortened graphene nanoribbons have aspect ratios of less than about 5. In other cases, shortened graphene nanoribbons have aspect ratios of less than about 3, or less than about 2. According to theoretical predictions, single-atomic and multiple-atomic layer graphene nanoribbons have a high surface energy that is thought to prevent their growth directly from the gas phase, even with proper nucleation. The failure to grow graphene nanoribbons directly from the gas phase is thought to be due to their tendency either to stack into graphite crystals or to fold into carbon nanotubes or similar closed structures. Although a strain energy barrier results from the curvature of the carbon nanotubes, the strain energy of the carbon nanotubes is less than the surface energy of the graphene sheets. Hence, carbon nanotubes are a preferred gas phase reaction product. The transverse edges of the graphene nanoribbon are substantially smooth. The edge termination state has little effect on the thermal conductivity, since there is little difference in thermal conductivity between zigzag-edged and armchair-edged graphene nanoribbons. However, the thermal conductivity depends strongly upon the nanoribbon length. More specifically, the thermal conductivity increases with increasing nanoribbon length due to the reduced probability of phonon scattering from grain boundaries. This is because the mean free path of phonons in graphene, which can be up to 700 nanometers at room temperature as noted above, is very large compared to the dimensions of the graphene nanoribbon. As a result, the length of the graphene nanoribbon is vital in determining the thermal conductivity. Consequently, the

length of the graphene nanoribbon is an important factor affecting the thermal properties, and must be taken into account so as to provide more accurate predictions about the thermal conductivity.

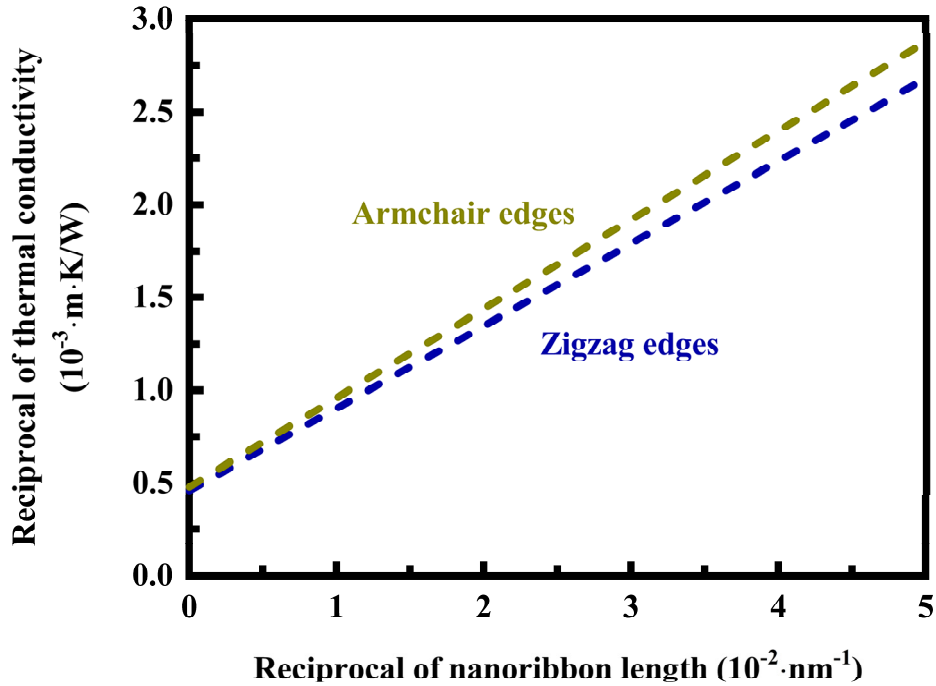


Figure 4. Effect of nanoribbon length on the thermal conductivity of the monolayer graphene nanoribbon with different transverse edge termination states.

The low-resolution scanning electron micrographs of the graphene nanoribbons are illustrated in Figure 5 for research purposes of thermal transport characteristics. The graphene nanoribbons have aspect ratios of at least 5 and the average aspect ratio of the graphene nanoribbons in the plurality of nanoribbons is at least 10 and, in some cases, at least 20. The graphene nanoribbons comprise two edges that run substantially parallel along the length of the nanoribbon and they have the armchair crystallographic direction of graphene running parallel to the nanoribbon edges. They have carbon-carbon bonds running parallel to the long nanoribbon axis. Because the graphene nanoribbons are grown, rather than patterned lithographically from graphene sheets, they are formed with atomically smooth edges. The degree of edge smoothness can be characterized by the average root mean square roughness of the edges of the nanoribbons in the array. The rms edge roughness along the length of a nanoribbon can be measured using scanning tunneling microscopy. The average rms edge roughness for the nanoribbons in a nanoribbon array will vary since longer nanoribbons within the array will tend to have rougher edges. Graphene nanoribbons outperform conventional materials and lead to next-generation technologies. Graphene nanoribbons offer tremendous promise for providing enhanced thermal transport performance. However, the full potential of graphene nanoribbons in such applications has not been realized. A major challenge facing graphene nanoribbon-based devices is that scalable approaches to create high-quality graphene nanoribbons with atomically-smooth edges are lacking. Conventional, top-down techniques in which graphene nanoribbons are etched from continuous graphene sheets result in structures with rough, disordered edges that are riddled with defects, which significantly degrade graphene's exceptional properties. This blunt top-down etching can be avoided by synthesizing nanoribbons from the bottom-up. For instance, organic synthesis can yield ribbons with smooth edges, defined widths, and complex architectures. However, organic synthesis forms short nanoribbons and is not adapted to technologically relevant substrates, such as insulators or semiconductors, limiting its potential for commercial development. Optionally, nucleation sites can be introduced into or onto the germanium growth surface in order to control the locations at which graphene nanoribbon growth originates and the time at which graphene nanoribbon growth begins.

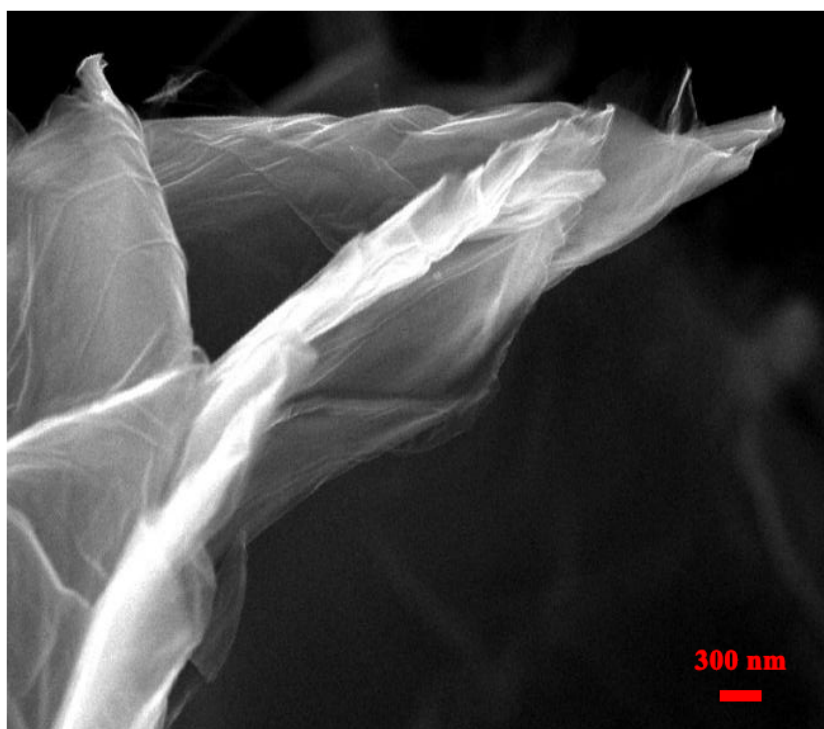


Figure 5. Low-resolution scanning electron micrographs of the graphene nanoribbons for research purposes of thermal transport characteristics.

The high-resolution scanning electron micrographs of the graphene nanoribbons are illustrated in Figure 6 for research purposes of thermal transport characteristics. The methods for preparing graphene nanoribbons described herein take place either in a liquid medium or on a surface. Without being bound by theory or mechanism, it is thought that when a free-standing graphene sheet is in solution, the excess surface energy may be stabilized by solvation energy such that folding into a carbon nanotube becomes energetically unfavorable. As a result of the solvation energy, the reverse process of longitudinally opening a carbon nanotube into a graphene nanoribbon becomes energetically favorable in an appropriate liquid medium. According to current understanding, the oxidative longitudinal opening of carbon nanotubes appears to occur along a line to afford predominantly straight-edged oxidized graphene nanoribbons. Graphene nanoribbons may be incorporated into organic and inorganic matrices such as, for example, polymer matrices. The polymer matrices can include, without limitation, thermoplastic and thermosetting polymer matrices. Incorporation of graphene nanoribbons may improve mechanical properties of the polymer composites. In some cases, polymer membranes including graphene nanoribbons may be prepared which are useful for fluid separations, antistatic applications, or electromagnetic shielding materials. The graphene nanoribbons may be dispersed as individuals in the polymer matrices. The graphene nanoribbons may also be aggregated together in two or more layers in the polymer matrices. The graphene nanoribbons may be covalently bonded to the polymer matrices. For example, carboxylic acid groups of graphene nanoribbons may be utilized for making cross-linked polymer composites in which the graphene nanoribbons are covalently bonded to the polymer matrix. Other functional groups in the graphene nanoribbons may be utilized as well for making cross-linked polymer composites. In other cases, the graphene nanoribbons are not covalently bonded to the polymer matrices. As a non-limiting example of composite materials, reinforced rubber composites including graphene nanoribbons may be used to manufacture gaskets and seals with improved tolerance to explosive decompression. The graphene nanoribbons can be deposited from a mixture of methane gas and hydrogen gas. By varying the composition of the precursor gas mixture during growth, the duration of the growth time, and the growth temperature, the graphene nanoribbon

width, length, and aspect ratio can be controlled. This control over the nanoribbon structure makes it possible to tune the graphene properties. For example, graphene undergoes a metallic-to-semiconducting transition as the nanoribbon width decreases, wherein the induced bandgap is inversely proportional to the nanoribbon width. Therefore, the present approach makes it possible to control the width of the nanoribbons and, therefore, to tailor their electronic structure. By tuning the precursor composition and growth time, nanoribbons with widths below the current lithography resolution can be achieved. Key parameters for realizing anisotropic growth are the mole fractions of the precursor molecules and the carrier molecules used in the chemical vapor deposition gas mixture, where the mole fractions can be adjusted by adjusting the partial pressures of the precursor and carrier gases. However, these parameters are not independent, so the optimum value for one of the parameters will depend on the others. The growth time also plays a role in determining the dimensions of the chemical vapor deposition-grown graphene nanoribbons. Generally, as growth time is decreased, narrower, shorter nanoribbons are formed. Therefore, by tuning the duration of the growth time and the ratio of precursor gas to carrier gas in the gas mixture, nanoribbons with desired lengths and widths can be selectively grown using bottom-up chemical vapor deposition growth. The optimum conditions for achieving anisotropic graphene growth may vary somewhat depending upon the laboratory conditions. For example, in a cleaner environment, the growth rate at a given set of conditions would be expected to be slower than in a dirtier environment. Therefore, to achieve the same low growth rate observed under standard laboratory conditions in a cleaner system, such as a clean room, a higher methane mole fraction and a lower hydrogen mole fraction could be used.



Figure 6. High-resolution scanning electron micrographs of the graphene nanoribbons for research purposes of thermal transport characteristics.

The effect of temperature on the thermal conductivity of the monolayer graphene nanoribbon is illustrated in Figure 7 with different transverse edge termination states. Graphene is a two-dimensional carbon allotrope, the electronic, and magnetic properties of which can be tuned by engineering two-dimensional graphene sheets into one-dimensional structures with confined width, known as graphene nanoribbons. The properties of graphene nanoribbons are highly dependent on their width and edge structure. Graphene nanoribbons possess a number of useful properties, including, for example, beneficial electrical properties. Unlike carbon nanotubes, which can be metallic, semi-metallic or semiconducting depending on their chiral geometry and diameter, the electrical properties of graphene nanoribbons are governed by their width and their edge configurations and functionalization. For example, graphene nanoribbons of less than about 10 nanometers in width are semiconductors, whereas similar graphene nanoribbons having a width greater than about 10 nanometers are metallic or semi-metallic conductors. The edge configurations of graphene nanoribbons having an armchair or zigzag arrangement of carbon atoms, along with the terminal edge functional groups, are also calculated to affect the transmission of electron carriers. Such armchair and zigzag arrangements are analogous to those defined in carbon nanotubes. In addition to the electrical properties, graphene nanoribbons maintain many of the desirable mechanical properties that carbon nanotubes and graphene sheets also possess. Various methods for making graphene sheets are known, including, for example, adhesive tape exfoliation of individual graphene layers from graphite, chemical-based exfoliation of graphene layers from graphite, and chemical vapor deposition processes, each process providing on the order of picogram quantities of graphene [41, 42]. Several lithographic and synthetic procedures have been developed for producing minuscule amounts of graphene nanoribbons [43, 44]. Microscopic quantities of graphene nanoribbons have been produced by partial encapsulation of carbon nanotubes in a polymer, followed by plasma etching to longitudinally cut the carbon nanotubes [45, 46]. Macroscopic quantities of graphene nanoribbons have also been produced by a chemical vapor deposition process [47, 48]. Graphene represents an atomically thin layer of carbon in which the carbon atoms reside at regular two-dimensional lattice positions within a single sheet or a few stacked sheets of fused six-membered carbon rings. In its various forms, this material has garnered widespread interest for use in a number of applications, primarily due to its favorable combination of high electrical and thermal conductivity values, good mechanical strength, and unique electronic properties. However, an advantage of graphene over carbon nanotubes is that graphene can generally be produced in bulk much more inexpensively than can the latter, thereby addressing perceived supply and cost issues that have been commonly associated with carbon nanotubes. Despite the fact that graphene is generally synthesized more easily than are carbon nanotubes, there remain issues with production of graphene in quantities sufficient to support various commercial operations. Scalability to produce large area graphene films represents a particular problem. The most scalable processes developed to date for making graphene films utilize chemical vapor deposition technology. Graphene nanoribbons prepared by these processes are typically characterized by multiple graphene layers with a kinked morphology and irregular atomic structure. Graphene nanoribbons are a single or a few layers of the well-known carbon allotrope graphitic carbon, which possesses exceptional electrical and physical properties which may lead to various applications. Graphene nanoribbons structurally have high aspect ratio with length being much longer than the width or thickness. Graphene nanoplatelets are similar to graphene nanoribbons except that the length is in the micron or sub-micron range and hence graphene nanoplatelets lack the high aspect ratio of graphene nanoribbons. Graphene nanoplatelets also possess many of the useful properties of carbon nanotubes and graphene nanoribbons. Graphene nanoribbons are prepared by chemical vapor deposition and from graphite using chemical processes. Most typically, graphene nanoribbons are prepared from carbon nanotubes by chemical unzipping and the quality of graphene nanoribbons depends the purity of the carbon nanotube starting material.

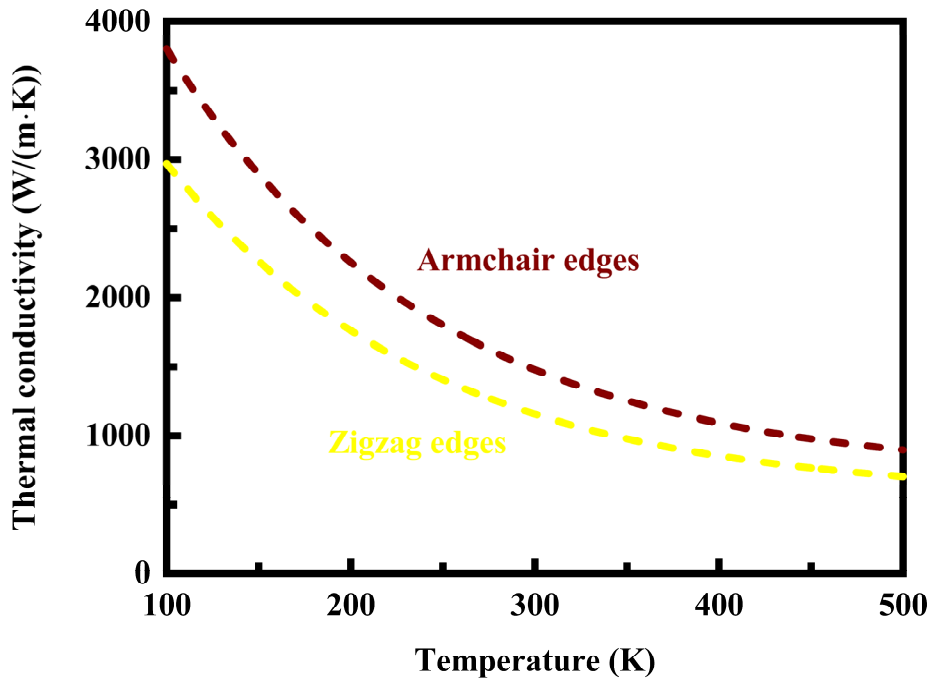


Figure 7. Effect of temperature on the thermal conductivity of the monolayer graphene nanoribbon with different transverse edge termination states.

The effect of the number of layers on the thermal conductivity of the monolayer graphene nanoribbon is illustrated in Figure 8 with different transverse edge termination states. Graphene typically refers to a material having less than about 10 graphitic layers. The graphitic layers are characterized by an infinite two-dimensional basal plane having a hexagonal lattice structure and various edge functionalities, which may include, for example, carboxylic acid groups, hydroxyl groups, epoxide groups and ketone groups. Graphene nanoribbons are a special class of graphene, which are similarly characterized by a two-dimensional basal plane, but with a large aspect ratio of their length to their width. In this regard, graphene nanoribbons bear similarity to carbon nanotubes, which have a comparable large aspect ratio defined by one or more layers of graphene sheets rolled up to form a cylinder. The graphene nanoribbons can include various layers. For instance, the graphene nanoribbons may include a single layer. In some cases, the graphene nanoribbons may include a plurality of layers. In some cases, the graphene nanoribbons include from about one layer to about eight layers. In some cases, the graphene nanoribbons include from about second layers to about ten layers. In some cases, the graphene nanoribbon layers have interlayer spacings of more than about 0.2 nanometers. In some cases, the graphene nanoribbon layers have interlayer spacings of 0.34 nanometers or larger. The graphene nanoribbons may be derived from various carbon sources. For instance, the graphene nanoribbons may be derived from carbon nanotubes, such as multi-walled carbon nanotubes. In some cases, the graphene nanoribbons are derived through the longitudinal splitting of carbon nanotubes. Various methods may be used to split carbon nanotubes to form graphene nanoribbons. Carbon nanotubes may be split by exposure to potassium, sodium, lithium, alloys thereof, metals thereof, salts thereof, and combinations thereof. For instance, the splitting may occur by exposure of the carbon nanotubes to a mixture of sodium and potassium alloys, a mixture of potassium and naphthalene solutions, and combinations thereof. In some cases, the graphene nanoribbons are made by the longitudinal splitting of carbon nanotubes using oxidizing agents or by the longitudinal opening of carbon nanotubes. The thermally conductive materials may also utilize various graphene nanoribbons. For instance, the graphene nanoribbons include, without limitation, functionalized graphene nanoribbons, pristine graphene nanoribbons, doped graphene nanoribbons, graphene oxide nanoribbons, reduced graphene oxide nanoribbons, reduced graphene oxide flakes, and combinations thereof.

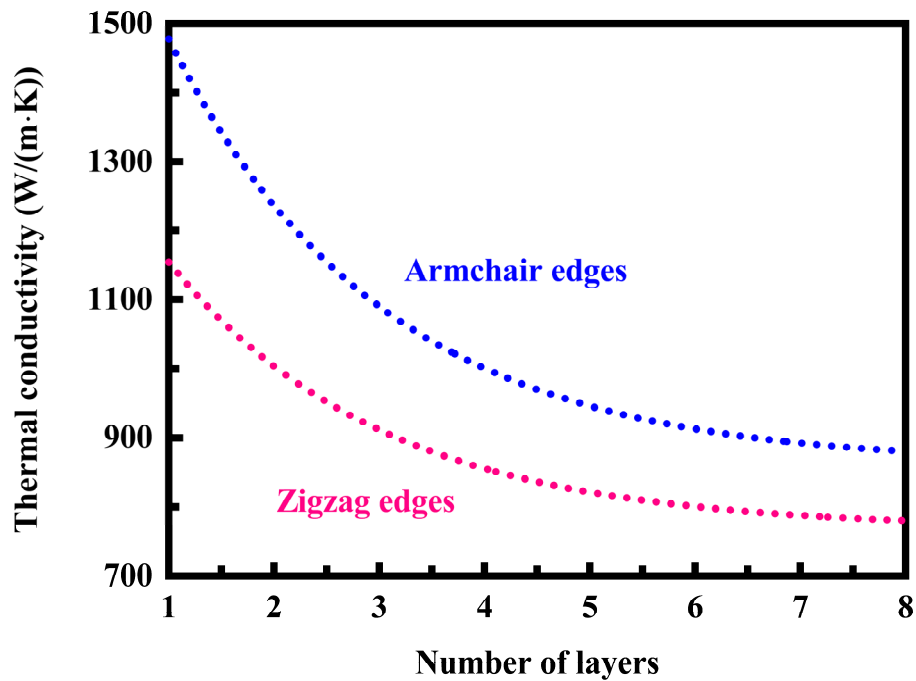


Figure 8. Effect of the number of layers on the thermal conductivity of the monolayer graphene nanoribbon with different transverse edge termination states.

4. Conclusions

The present study is focused primarily upon the thermal transport characteristics of graphene nanoribbons. The thermal transport characteristics of graphene nanoribbons are studied using molecular dynamics simulations and by experimental measurements. A specific heat flux is imposed through the graphene nanoribbon. The graphene nanoribbon is considered as a single layer of carbon atoms with each atom bound to three neighbors in a honeycomb structure. The thermal conductivity is determined from the temperature gradient obtained and the heat flux imposed. The thermal properties of the graphene nanoribbon with different lengths are investigated to determine the structure factors limiting the heat transfer process. The present study aims to provide a fundamental understanding of the thermal transport properties of graphene nanoribbons. Particular emphasis is placed upon the effect of various factors on the thermal conductivity of graphene nanoribbons under different conditions. The major conclusions are summarized as follows:

- The mean free path of phonons depends on the nanoribbon structure and dimensions.
- The thermal conductivity increases with increasing nanoribbon length.
- Graphene nanoribbons offer tremendous promise for providing enhanced transport performance.
- Graphene undergoes a metallic-to-semiconducting transition as the nanoribbon width decreases.
- The properties of graphene nanoribbons are highly dependent on their width and edge structure.
- The graphene nanoribbons can be derived through the longitudinal splitting of carbon nanotubes.

References

- [1] J.M. Carlsson and M. Scheffler. Structural, electronic, and chemical properties of nanoporous carbon. *Physical Review Letters*, Volume 96, Issue 4, 2006, Article Number: 046806.
- [2] T.O. Wehling, E. Şaşıoğlu, C. Friedrich, A.I. Lichtenstein, M.I. Katsnelson, and S. Blügel. Strength of effective coulomb interactions in graphene and graphite. *Physical Review Letters*, Volume 106, Issue 23, 2011, Article Number: 236805.

- [3] R.E. Smalley. Discovering the fullerenes. *Reviews of Modern Physics*, Volume 69, Issue 3, 1997, Pages 723-730.
- [4] P. Ayala, R. Arenal, A. Loiseau, A. Rubio, and T. Pichler. The physical and chemical properties of heteronanotubes. *Reviews of Modern Physics*, Volume 82, Issue 2, 2010, Pages 1843-1885.
- [5] A.M. Marconnet, M.A. Panzer, and K.E. Goodson. Thermal conduction phenomena in carbon nanotubes and related nanostructured materials. *Reviews of Modern Physics*, Volume 85, Issue 3, 2013, Pages 1295-1326.
- [6] K.L. Klein, A.V. Melechko, T.E. McKnight, S.T. Retterer, P.D. Rack, J.D. Fowlkes, D.C. Joy, and M.L. Simpson. Surface characterization and functionalization of carbon nanofibers. *Journal of Applied Physics*, Volume 103, Issue 6, 2008, Article Number: 061301.
- [7] S. Mrozowski. Zone structure of graphite. *Physical Review*, Volume 92, Issue 5, 1953, Pages 1320-1321.
- [8] J.C. Slonczewski and P.R. Weiss. Band structure of graphite. *Physical Review*, Volume 109, Issue 2, 1958, Pages 272-279.
- [9] H. Shioyama. The interactions of two chemical species in the interlayer spacing of graphite. *Synthetic Metals*, Volume 114, Issue 1, 2000, Pages 1-15.
- [10] C. Binns, S.H. Baker, C. Demangeat, and J.C. Parlebas. Growth, electronic, magnetic and spectroscopic properties of transition metals on graphite. *Surface Science Reports*, Volume 34, Issues 4-5, 1999, Pages 107-170.
- [11] P.M. Adams, H.A. Katzman, G.S. Rellick, and G.W. Stupian. Characterization of high thermal conductivity carbon fibers and a self-reinforced graphite panel. *Carbon*, Volume 36, Issue 3, 1998, Pages 233-245.
- [12] M. Kerford and R.P. Webb. An investigation of the thermal profiles induced by energetic carbon molecules on a graphite surface. *Carbon*, Volume 37, Issue 5, 1999, Pages 859-864.
- [13] R.S. Rubino and E.S. Takeuchi. The study of irreversible capacity in lithium-ion anodes prepared with thermally oxidized graphite. *Journal of Power Sources*, Volumes 81-82, 1999, Pages 373-377.
- [14] J. Gibkes, B.K. Bein, D. Krüger, and J. Pelzl. Thermophysical characterization of fine-grain graphites based on thermal waves. *Carbon*, Volume 31, Issue 5, 1993, Pages 801-807.
- [15] P.G. Klemens and D.F. Pedraza. Thermal conductivity of graphite in the basal plane. *Carbon*, Volume 32, Issue 4, 1994, Pages 735-741.
- [16] M.S. Seehra and A.S. Pavlovic. X-Ray diffraction, thermal expansion, electrical conductivity, and optical microscopy studies of coal-based graphites. *Carbon*, Volume 31, Issue 4, 1993, Pages 557-564.
- [17] D. Angermeier, R. Monna, A. Slaoui, and J.C. Muller. Analysis of thin film polysilicon on graphite substrates deposited in a thermal CVD system. *Journal of Crystal Growth*, Volume 191, Issue 3, 1998, Pages 386-392.
- [18] C.-C. Hung and J. Miller. Thermal conductivity of pristine and brominated highly graphitized pitch based carbon fibers. *Carbon*, Volume 25, Issue 5, 1987, Pages 679-684.
- [19] B. Kastelein, R.D.V. Bergen, H. Postma, H.C. Meijer, and F. Mathu. Thermal conductance of highly oriented pyrolytic graphite along the c-direction at very low temperatures including magnetic field effects. *Carbon*, Volume 30, Issue 6, 1992, Pages 845-850.
- [20] B.T. Kelly and K.E. Gilchrist. The basal thermal conductivity of highly oriented pyrolytic graphite as a function of degree of graphitization. *Carbon*, Volume 7, Issue 3, 1969, Pages 355-358.
- [21] V.J. Cee, D.L. Patrick, and T.P. Beebe. Unusual aspects of superperiodic features on highly oriented pyrolytic graphite. *Surface Science*, Volume 329, Issues 1-2, 1995, Pages 141-148.
- [22] F. Rodriguez-reinoso and P.A. Thrower. Microscopic studies of oxidized highly oriented pyrolytic graphites. *Carbon*, Volume 12, Issue 3, 1974, Pages 269-279.

- [23] J. Kim, D. Kim, K.W. Lee, E.H. Choi, S.J. Noh, H.S. Kim, and C.E. Lee. Proton-irradiation effects on the charge transport in highly oriented pyrolytic graphite. *Solid State Communications*, Volume 186, 2014, Pages 5-7.
- [24] H. Fredriksson, D. Chakarov, and B. Kasemo. Patterning of highly oriented pyrolytic graphite and glassy carbon surfaces by nanolithography and oxygen plasma etching. *Carbon*, Volume 47, Issue 5, 2009, Pages 1335-1342.
- [25] T. Scheike, P. Esquinazi, A. Setzer, and W. Böhlmann. Granular superconductivity at room temperature in bulk highly oriented pyrolytic graphite samples. *Carbon*, Volume 59, 2013, Pages 140-149.
- [26] D. Díaz-Fernández, J. Méndez, A.D. Campo, R.J.O. Mossaneck, M. Abbate, M.A. Rodríguez, G. Domínguez-Cañizares, O. Bomati-Miguel, A. Gutiérrez, and L. Soriano. Nanopatterning on highly oriented pyrolytic graphite surfaces promoted by cobalt oxides. *Carbon*, Volume 85, 2015, Pages 89-98.
- [27] M.D. Shirk and P.A. Molian. Ultra-short pulsed laser ablation of highly oriented pyrolytic graphite. *Carbon*, Volume 39, Issue 8, 2001, Pages 1183-1193.
- [28] J. Humlíček, A. Nebojsa, F. Munz, M. Miric, and R. Gajic. Infrared ellipsometry of highly oriented pyrolytic graphite. *Thin Solid Films*, Volume 519, Issue 9, 2011, Pages 2624-2626.
- [29] E. Pollmann, P. Ernst, L. Madauß, and M. Schleberger. Ion-mediated growth of ultra thin molybdenum disulfide layers on highly oriented pyrolytic graphite. *Surface and Coatings Technology*, Volume 349, 2018, Pages 783-786.
- [30] Z.-H. Wang, K. Kanai, K. Iketaki, Y. Ouchi, and K. Seki. Epitaxial growth of p-sexiphenyl film on highly oriented pyrolytic graphite surface studied by scanning tunneling microscopy. *Thin Solid Films*, Volume 516, Issue 9, 2008, Pages 2711-2715.
- [31] N. Bajales, M. Ávila, V. Galván, and P.G. Bercoff. Multi-characterization of electron-induced defects in highly oriented pyrolytic graphite. *Current Applied Physics*, Volume 16, Issue 3, 2016, Pages 421-427.
- [32] D.S. Martin, P. Weightman, and J.T. Gauntlett. The adsorption of n-hexadecane onto highly oriented pyrolytic graphite studied by atomic force microscopy. *Surface Science*, Volume 398, Issue 3, 1998, Pages 308-317.
- [33] A.M. Borisov, E.S. Mashkova, A.S. Nemov, and E.S. Parilis. Effect of radiation damage on ion-induced electron emission from highly oriented pyrolytic graphite. *Vacuum*, Volume 80, Issue 4, 2005, Pages 295-301.
- [34] M.A. Mannan, H. Noguchi, T. Kida, M. Nagano, N. Hirao, and Y. Baba. Growth and characterization of stoichiometric BCN films on highly oriented pyrolytic graphite by radiofrequency plasma enhanced chemical vapor deposition. *Thin Solid Films*, Volume 518, Issue 15, 2010, Pages 4163-4169.
- [35] D.S. Martin, P. Weightman, and J.T. Gauntlett. The evaporation of n-hexadecane from highly oriented pyrolytic graphite studied by atomic force microscopy. *Surface Science*, Volume 417, Issues 2-3, 1998, Pages 390-405.
- [36] Y. Baba, K. Nagata, S. Takahashi, N. Nakamura, N. Yoshiyasu, M. Sakurai, C. Yamada, S. Ohtani, and M. Tona. Surface modification on highly oriented pyrolytic graphite by slow highly charged ions. *Surface Science*, Volume 599, Issues 1-3, 2005, Pages 248-254.
- [37] R.S. Holt. Electron correlation effects in the momentum distribution of highly oriented pyrolytic graphite. *Solid State Communications*, Volume 59, Issue 5, 1986, Pages 321-323.
- [38] D.-Q. Yang, K.N. Piyakis, and E. Sacher. The manipulation of Cu cluster dimensions on highly oriented pyrolytic graphite surfaces by low energy ion beam irradiation. *Surface Science*, Volume 536, Issues 1-3, 2003, Pages 67-74.

- [39]E. Vetrivendan, R. Hareesh, and S. Ningshen. Synthesis and characterization of chemical vapour deposited pyrolytic graphite. *Thin Solid Films*, Volume 749, 2022, Article Number: 139180.
- [40]P. Touzain and A. Hamwi. De-intercalation and second intercalation of potassium into a highly oriented pyrolytic graphite. *Synthetic Metals*, Volume 23, Issues 1-4, 1988, Pages 127-132.
- [41]S. Kiddell, Y. Kazemi, J. Sorken, and H. Naguib. Influence of flash graphene on the acoustic, thermal, and mechanical performance of flexible polyurethane foam. *Polymer Testing*, Volume 119, 2023, Article Number: 107919.
- [42]R.P. Yali, A. Mehri, and M. Jamaati. Nonlinear thermal transport in graphene nanoribbon: A molecular dynamics study. *Physica A: Statistical Mechanics and its Applications*, Volume 610, 2023, Article Number: 128416.
- [43]J.C. Bi, H. Yun, M. Cho, M.-G. Kwak, B.-K. Ju, and Y. Kim. Thermal conductivity and mechanical durability of graphene composite films containing polymer-filled connected multilayer graphene patterns. *Ceramics International*, Volume 48, Issue 12, 2022, Pages 17789-17794.
- [44]H. Yun, D.G. Yang, J.C. Bi, M.-G. Kwak, and Y. Kim. Fabrication and properties of thermally conductive adhesive tapes containing multilayer graphene patterns. *Ceramics International*, Volume 48, Issue 22, 2022, Pages 34053-34058.
- [45]Z. Moradi, M. Vaezzadeh, and M. Saeidi. Temperature-dependent thermal expansion of graphene. *Physica A: Statistical Mechanics and its Applications*, Volume 512, 2018, Pages 981-985.
- [46]H. Rezania and M. Yarmohammadi. Dynamical thermal conductivity of bilayer graphene in the presence of bias voltage. *Physica E: Low-dimensional Systems and Nanostructures*, Volume 75, 2016, Pages 125-135.
- [47]K.K. Choudhary. Investigation of two-dimensional lattice thermal transport in bilayer graphene using phonon scattering mechanism. *Physica E: Low-dimensional Systems and Nanostructures*, Volume 58, 2014, Pages 106-110.
- [48]N. Usha, V. Subramanian, V.R.K. Murthy, and J. Sobhanadri. Microwave studies on some low stage graphite ferric chloride intercalation compound. *Materials Science and Engineering: B*, Volume 45, Issues 1-3, 1997, Pages 85-87.